Universität Stuttgart
Institut für Photogrammetrie (ifp)

DGPF

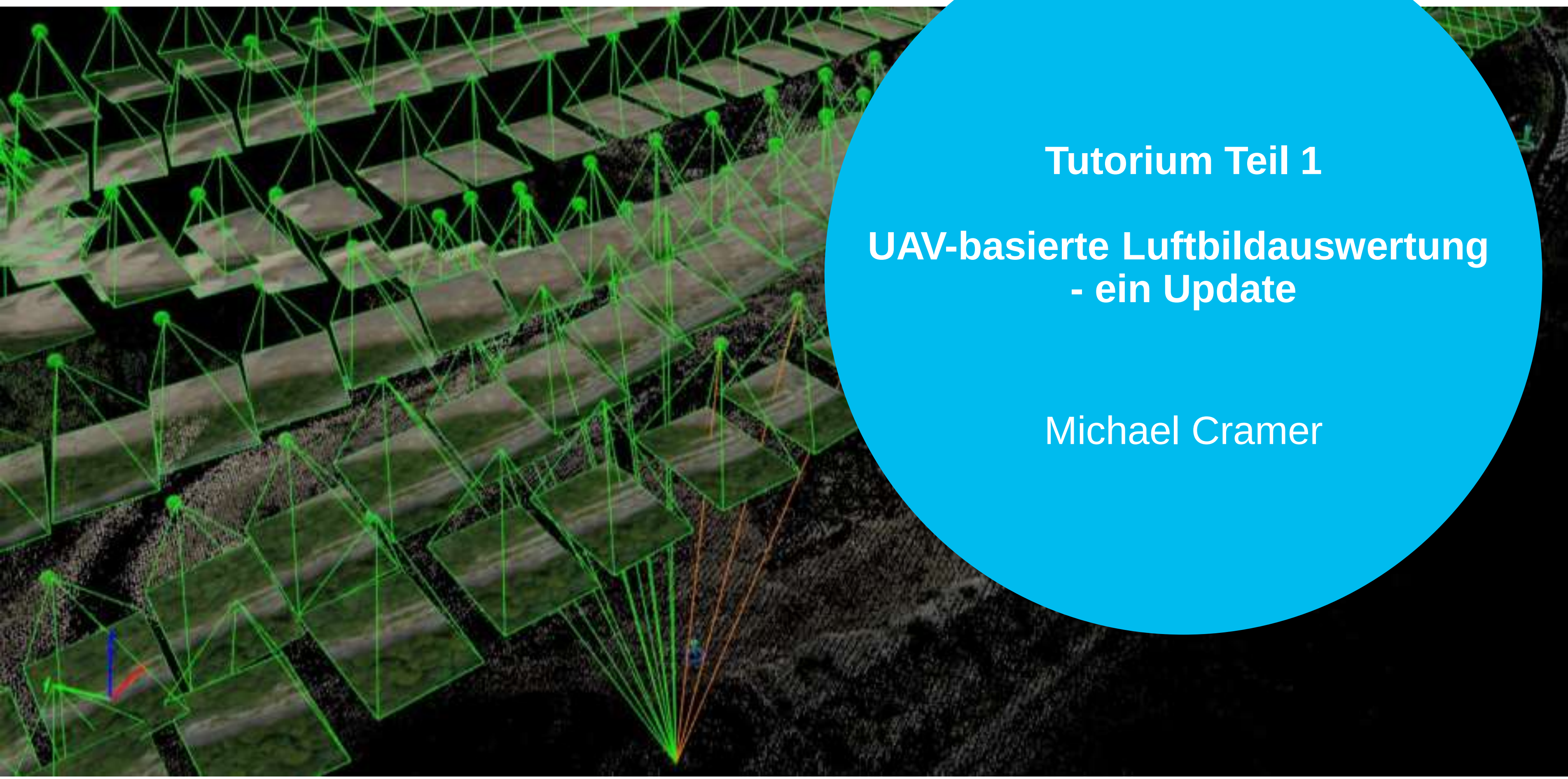

Tutorium Teil 1

UAV-basierte Luftbildauswertung - ein Update

Michael Cramer

Tutorium DGPF Jahrestagung Stuttgart 2019
Institut für Photogrammetrie, Universität Stuttgart, 04.03.2020

ifp

- Is UAV-based mapping so much different to regular flight campaigns?

- “With a little help from my friends” – using GNSS/inertial-based georeferencing for UAV-imagery – case study

- Are there further updates in the georeferencing of UAV-based imagery?
  - Extended AT with relative position and attitude control
  - Fast AT
  - Hybrid LiDAR & images georeferencing
  - Tightly coupling of GNSS/inertial data & image observations in one adjustment

Universität Stuttgart

DGPF

State-of-the-art in UAV-based mapping – an update

Is UAV-based mapping so much different to regular flight campaigns?

ifp

Use of UAV in Mapping / Photogrammetry

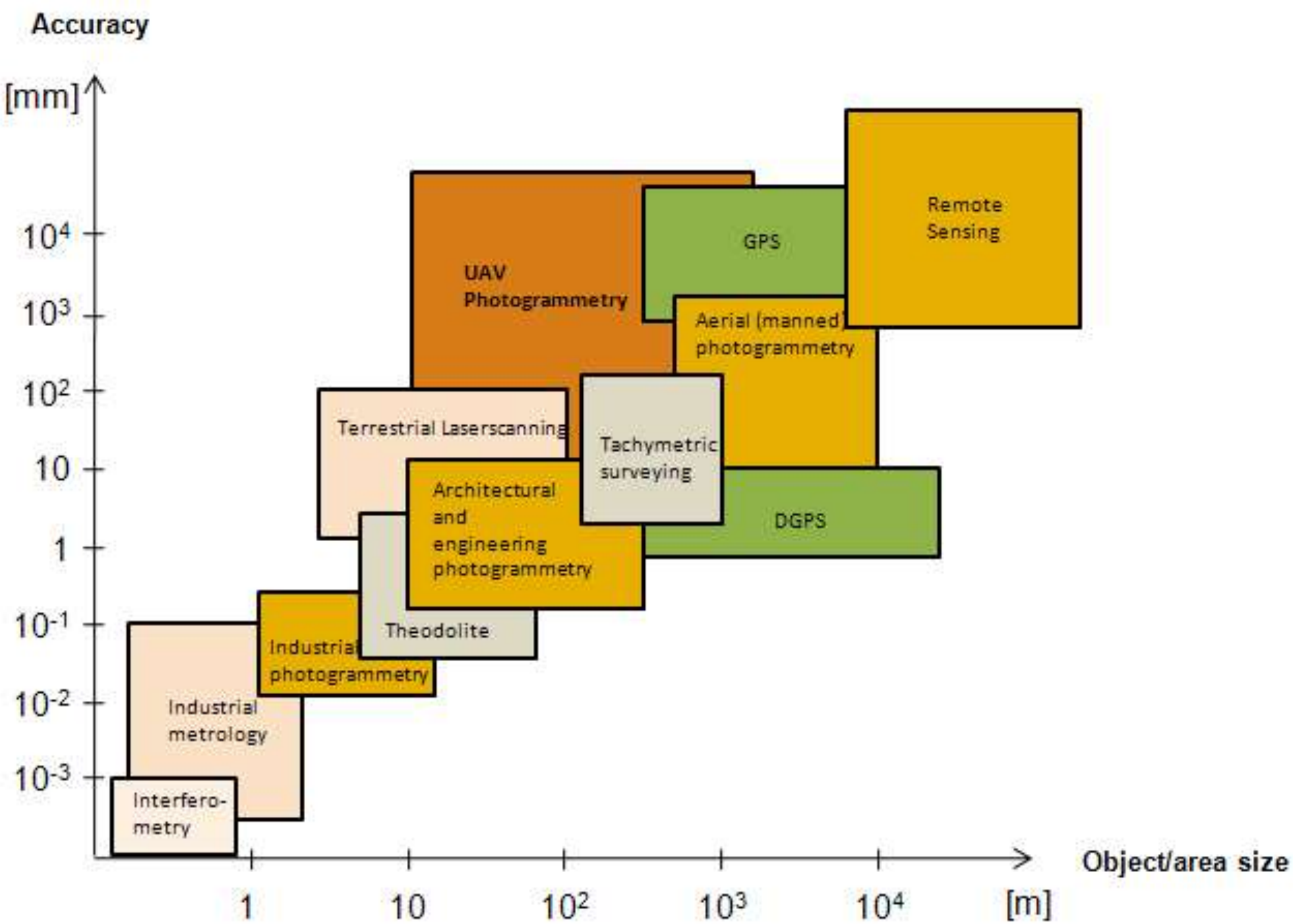

Manned vs. unmanned photo flights
Platforms & cameras

Platform

Camera

Block configurations: Manned platform

Orthomapping flights LGL BW

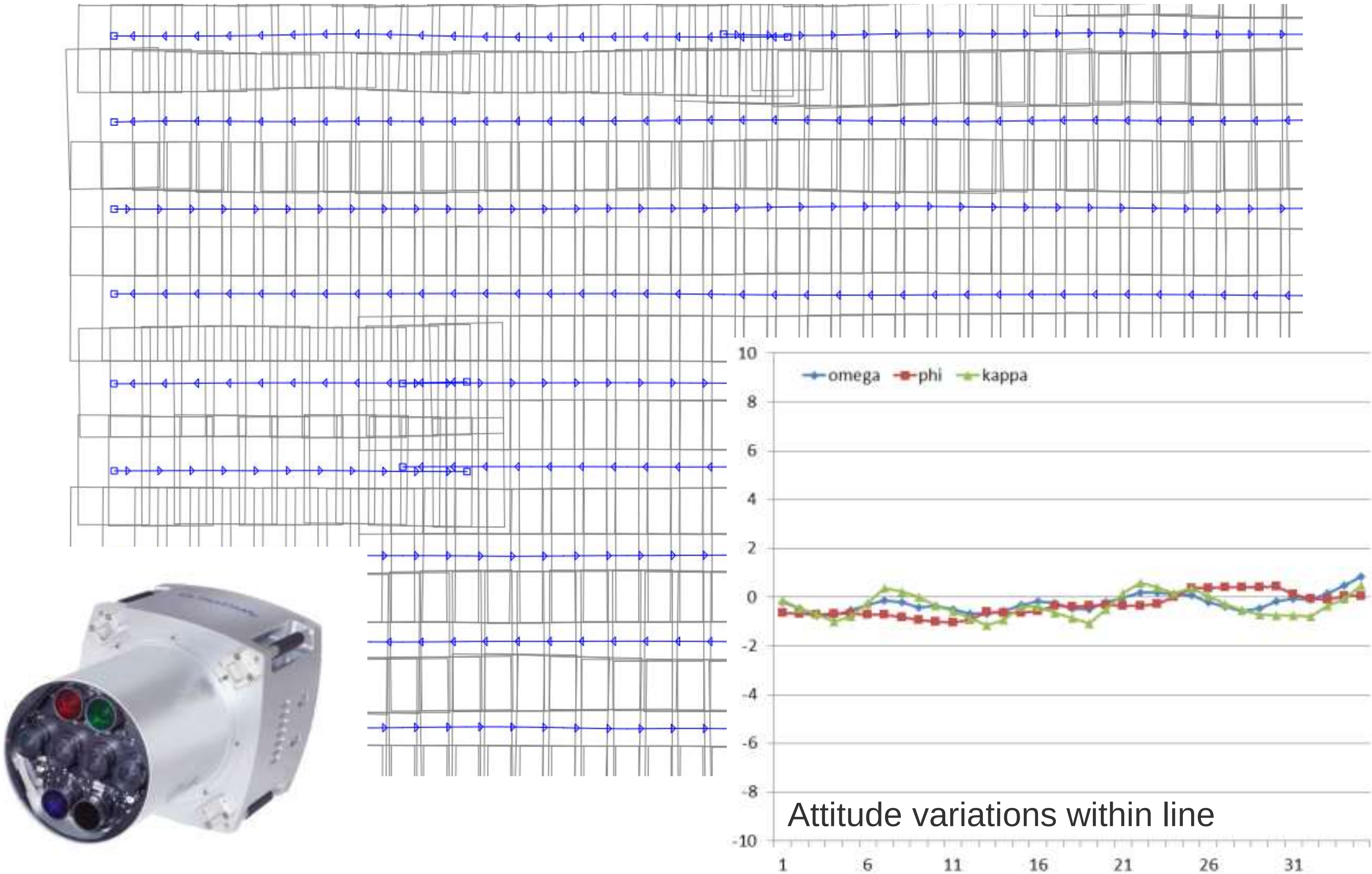

Block configurations: UAS – fixed wing

fixed wing
No camera stabilization

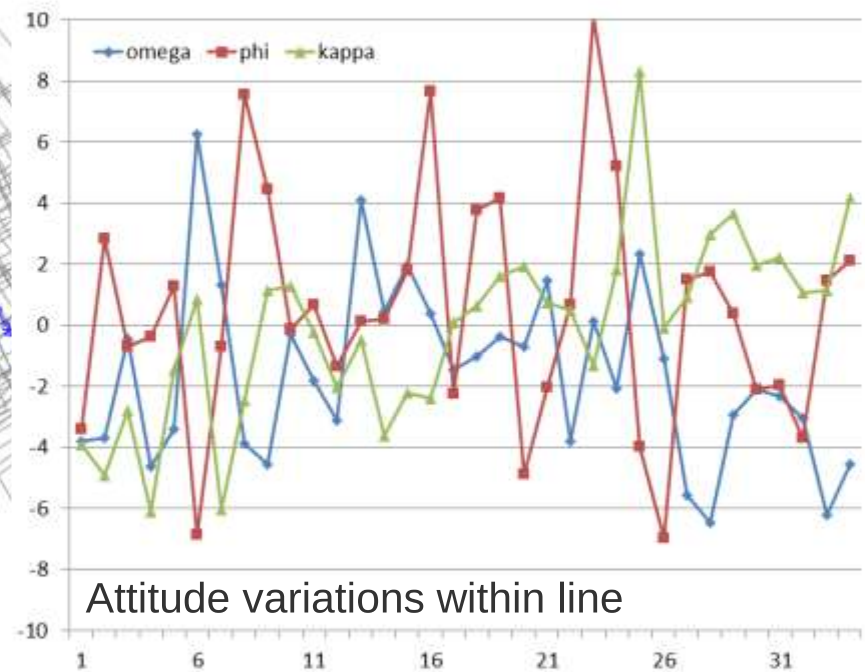

Block configurations: UAS – fixed wing

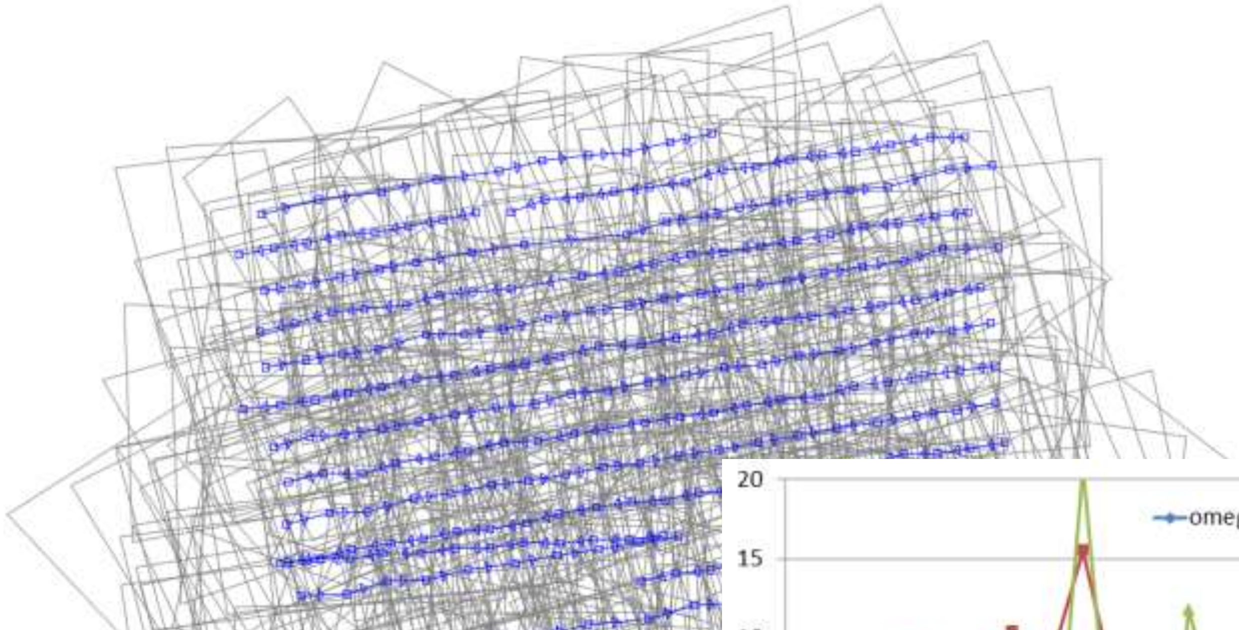

fixed wing
No camera stabilization

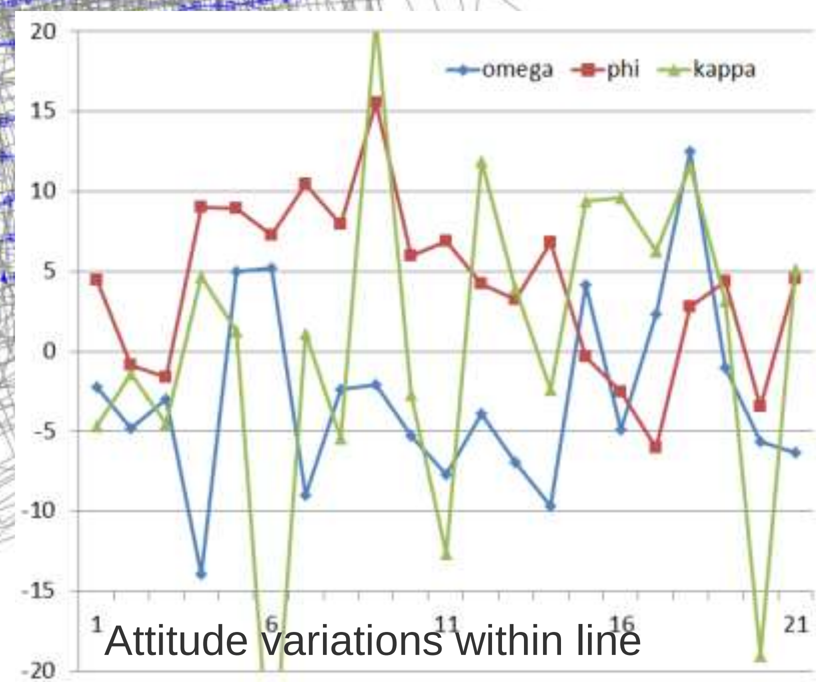

Notice: heavy wind gusts during flight.
Flight conditions close to limit!

Block configurations: UAS – rotary wing

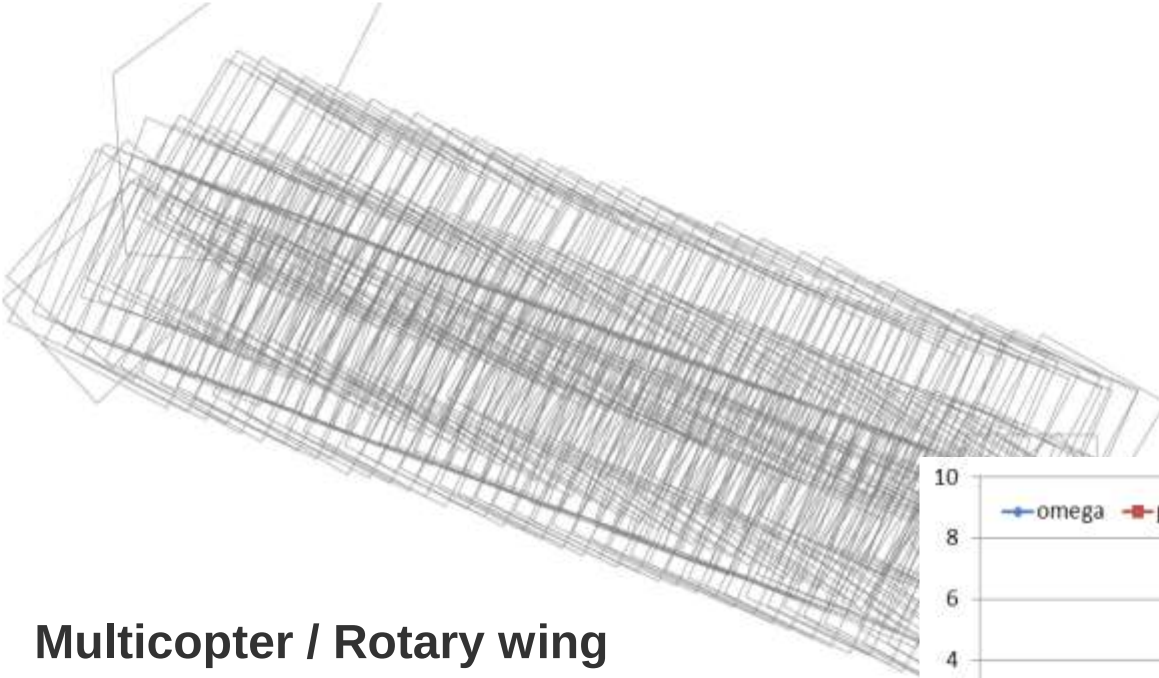

Multicopter / Rotary wing
Camera stabilization

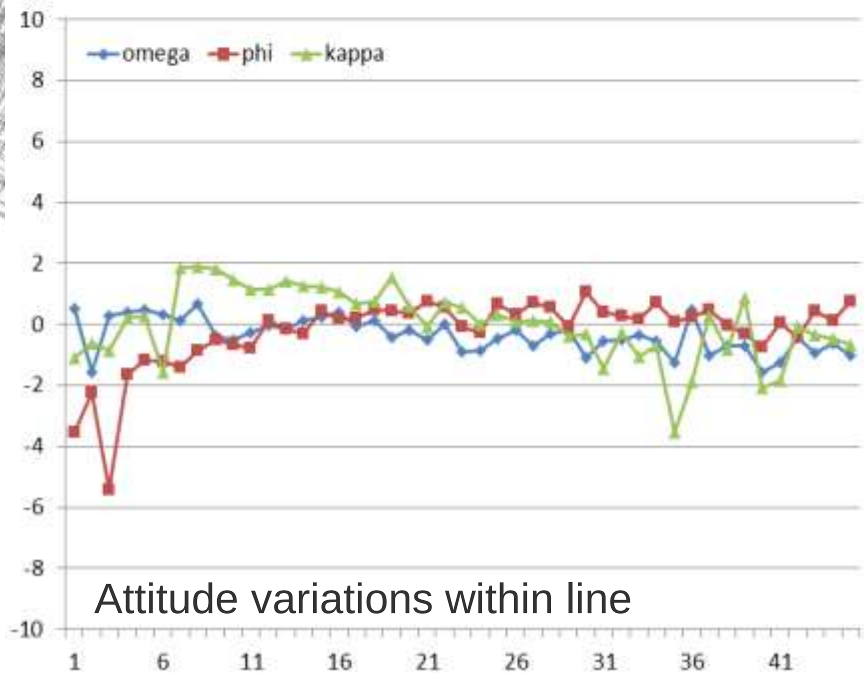

Attitude variations within line

Aerial Triangulation

Process chain

Initial Orientation / Set-up of Image Block

Orientation of image block

Transformation into object coordinate frame

camera calibration

Product generation DTM/DSM (Dense Matching) & Ortho

Aerial Triangulation (classical vs. UAV-based)

Standard-AT	Process chain	UAV
levelled camera High-precise GNSS/IMU	Initial Orientation / Set-up of Image Block	Larger off-nadir angles Less accurate attitudes > 0…20deg
"few" tie points (FBM/LSM)	Orientation of image block	many key points (SIFT)
GNSS supported AT (few) control points	Transformation into object coordinate frame	control points (except RTK & GNSS/IMU)
pre-calibrated cams + self-calibration (math. models)	camera calibration	Full in-situ camera calibration (physical models)
	Product generation DTM/DSM (Dense Matching) & Ortho	

Tie point extraction

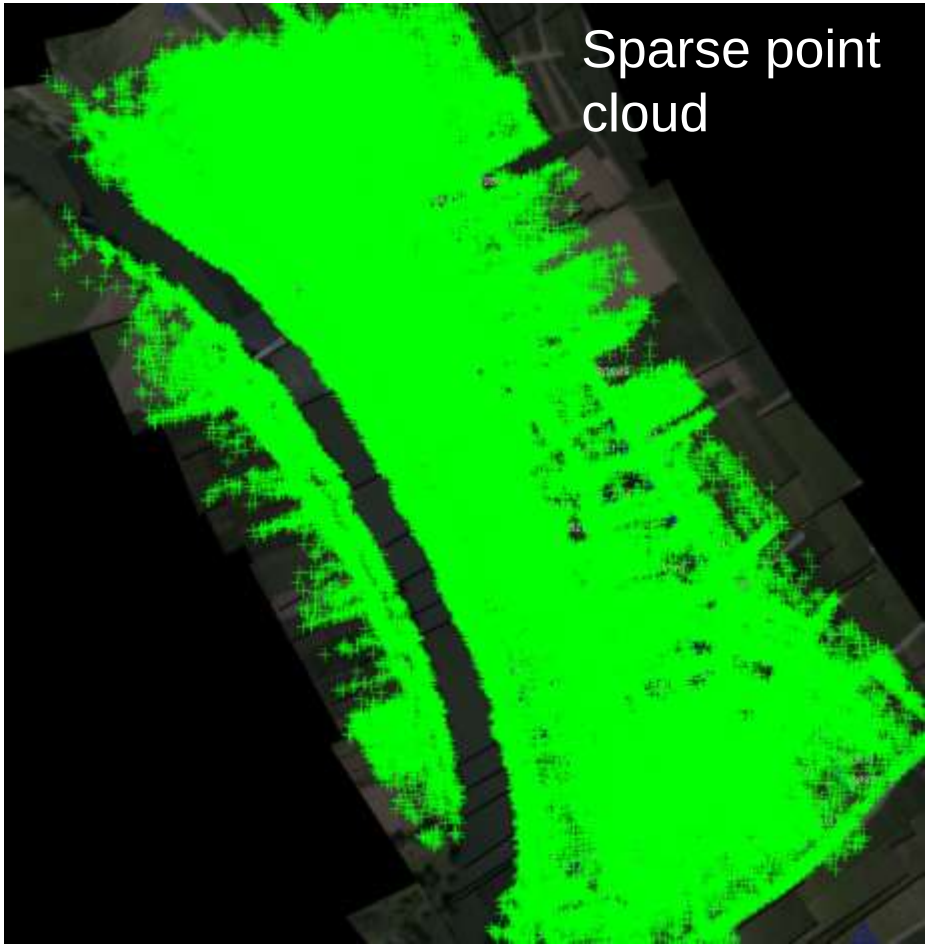

SIFT-Points (SfM Bundler)

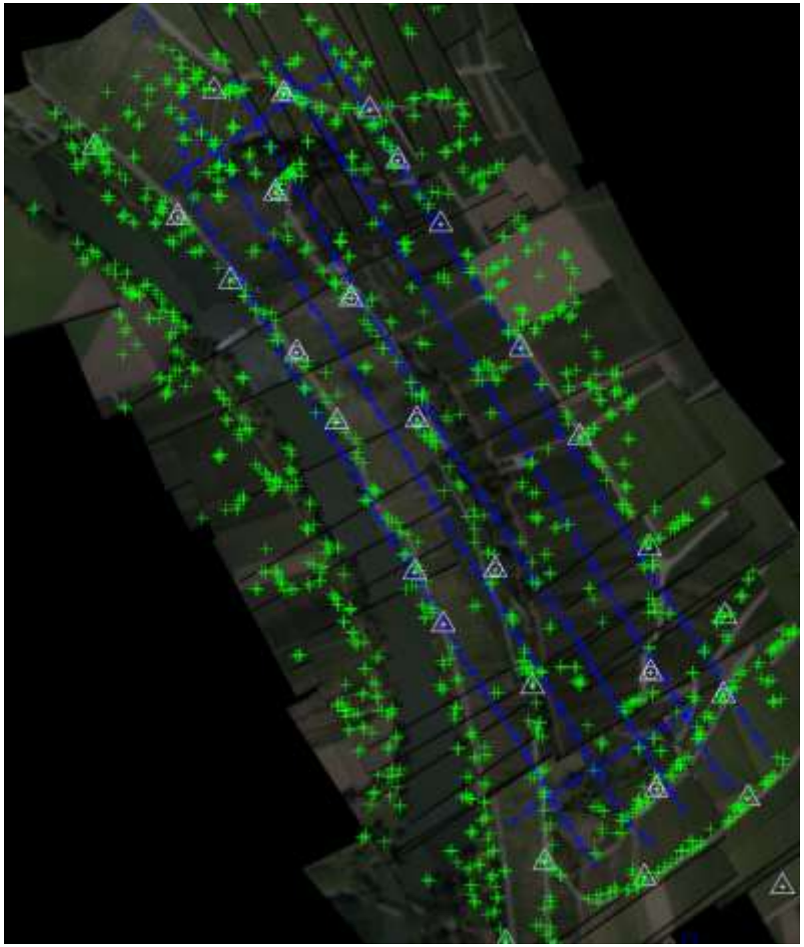

FBM/LSM points (inpho Match-AT)

Manned vs. unmanned photo flights
Mapping Camera vs. Bridge Camera

	Leica DMC III	Sony Alpha 7Rii
Image format	CMOS, 102 x 56 mm² 26112 x 15.000 pix @ 3.9 µm / 392 MPix	CMOS, 36 x 24 mm² 7952 x 5304 pix @ 4.5 µm / 42 MPix
Lens	Fixed lens, fix focus lens Multiple lens PAN&MS	interchangeable lens One lens only
Shutter	mechanical, **global**	electronical, **rolling**
Motion comp.	FMC (mechanical)	optical image stabilization
Dimensions Weight	622 x 497 x 460 mm 60kg (plus 6kg memory)	127 x 96 x 60 mm 625g (plus lens)

Rolling shutter – extreme sample

Rolling shutter

Source Pix4D

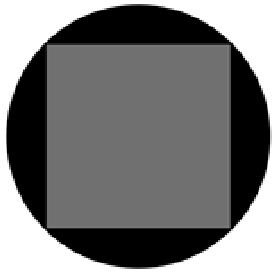

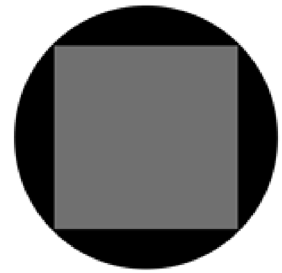

Global Shutter

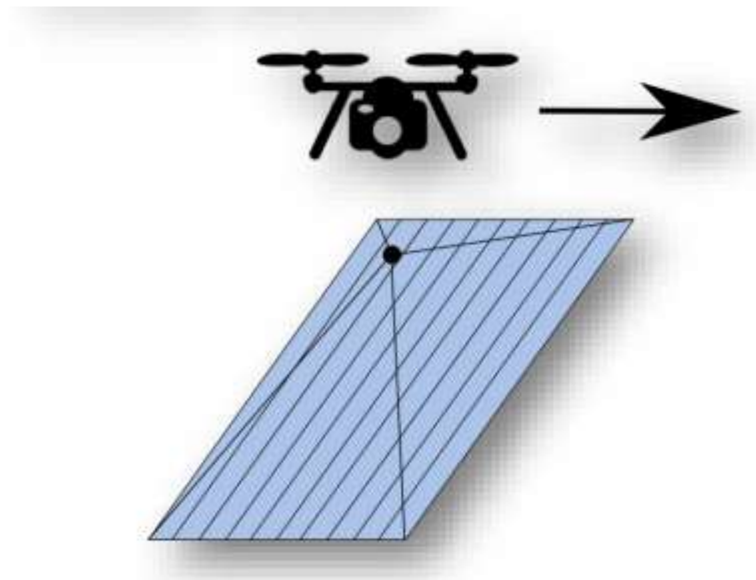

Rolling Shutter

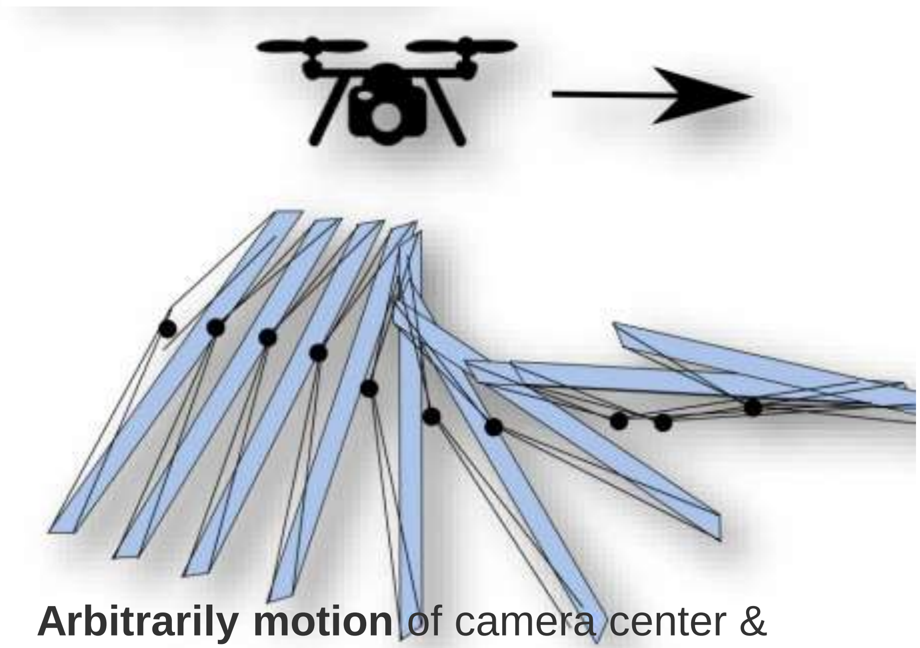

Arbitrarily motion of camera center & rotation over time

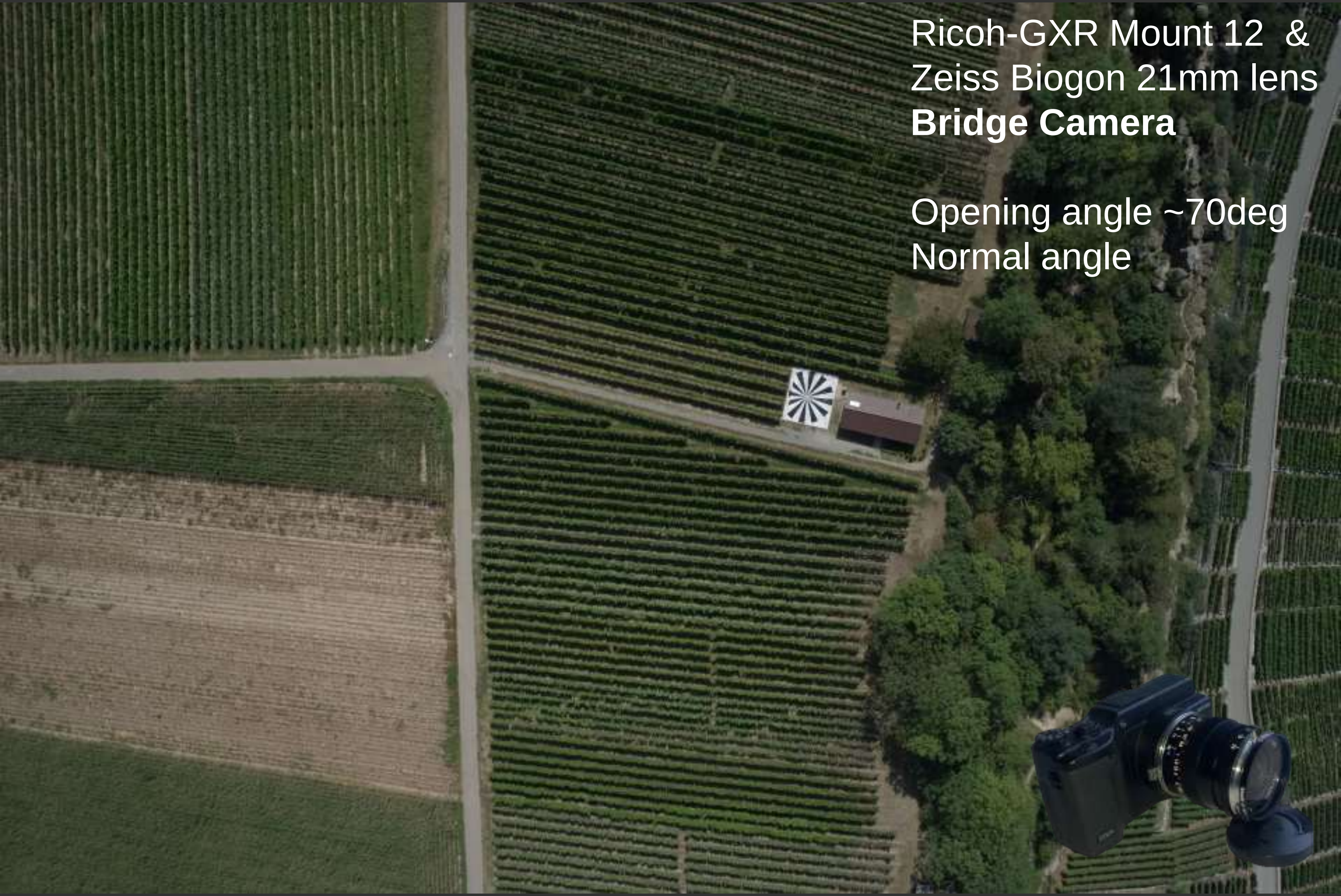
Ricoh-GXR Mount 12 &
Zeiss Biogon 21mm lens
Bridge Camera
Opening angle ~70deg
Normal angle

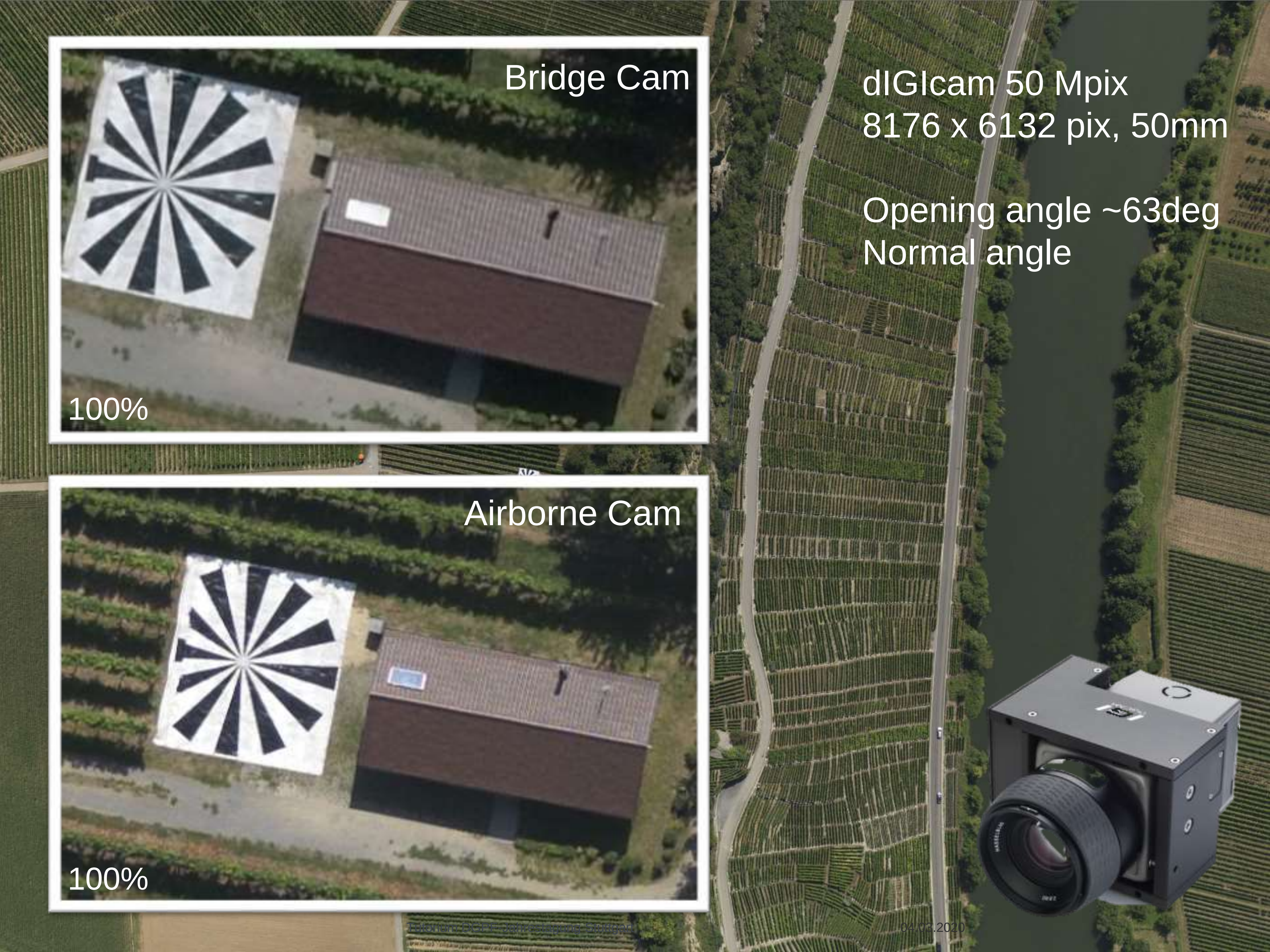
Bridge Cam
100%
Airborne Cam
100%
dIGIcam 50 Mpix
8176 x 6132 pix, 50mm
Opening angle ~63deg
Normal angle

Performance of camera – geometric resolution

Comparison Phase One iXM 100 & dji Phantom 4 RTK

DJI Phantom 4 RTK

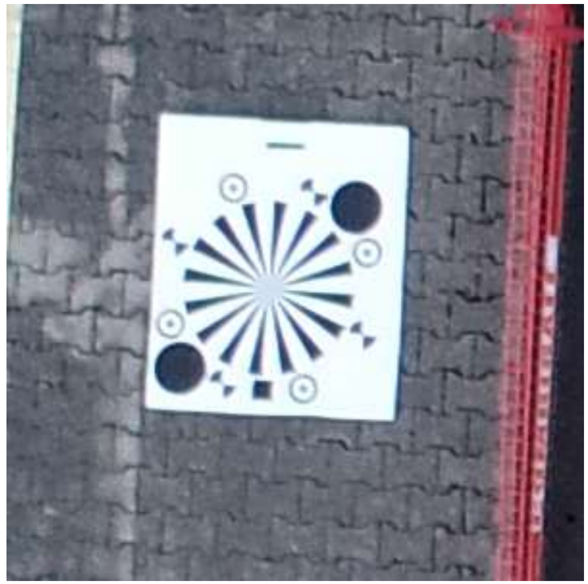

Phase One iXM-100

Samples:
Siemens star
in image center

	DJI Phantom 4 RTK		Phase One iXM-100	
Resolution MTF10	0.563 line/pix		0.769 line/pix	
GSD (nom.)	6.9 mm	178 %	5.0 mm	130 %
tGSD or GRD	12.3 mm		6.5 mm	

Performance of camera – geometric resolution

Comparison Phase One iXM 100 & dji Phantom 4 RTK

DJI Phantom 4 RTK

Sensor format 13.2 × 8.8mm²
Pixel count 5472 x 3648pix
Pixel size 2.41µm

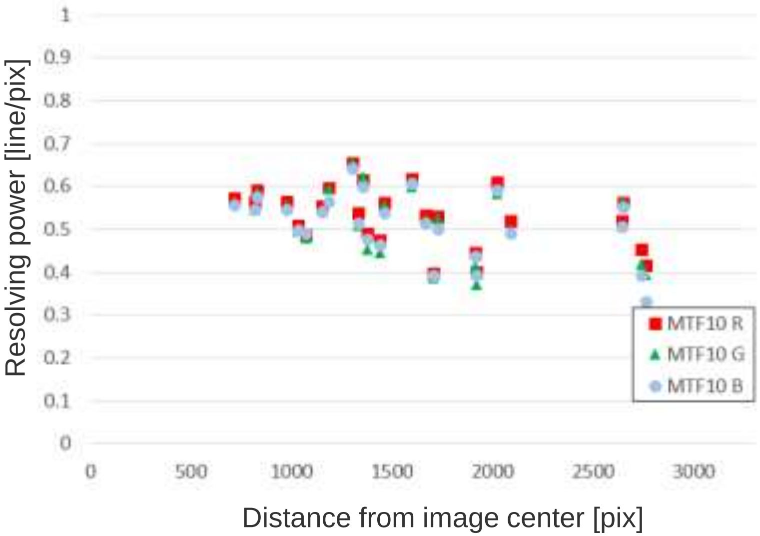

Phase One iXM-100 / 35mm lens

Sensor format 43.9 x 32.9 mm²
Pixel count 11664 x 8750pix
Pixel size 3.76µm

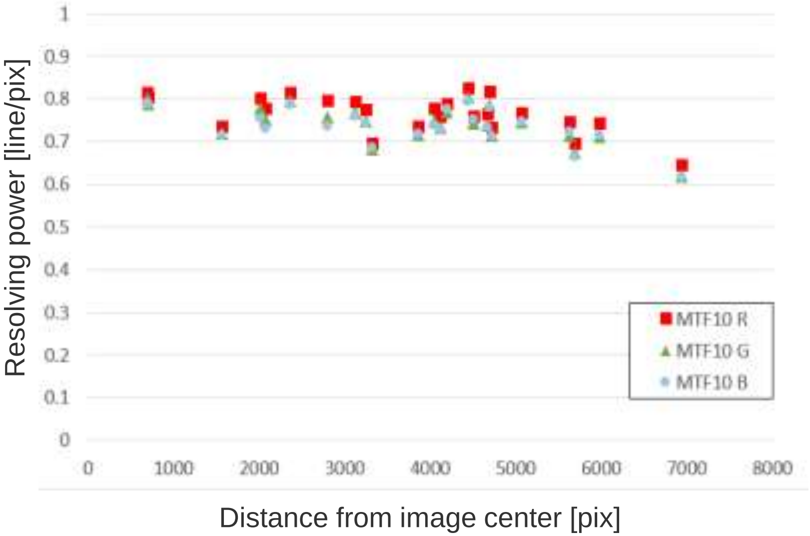

Questions & Comments ?!

- Is UAV-based mapping so much different to regular flight campaigns?

- "With a little help from my friends" – using GNSS/inertial-based georeferencing for UAV-imagery – case study

- Are there further updates in the georeferencing of UAV-based imagery?
  - Extended AT with relative position and attitude control
  - Fast AT
  - Hybrid LiDAR & images georeferencing
  - Tightly coupling of GNSS/inertial data & image observations in one adjustment

Universität Stuttgart

State-of-the-art in UAV-based mapping – an update

“With a little help from my friends” – using GNSS/inertial-based georeferencing for UAV-imagery – case study

Indirect georeferencing

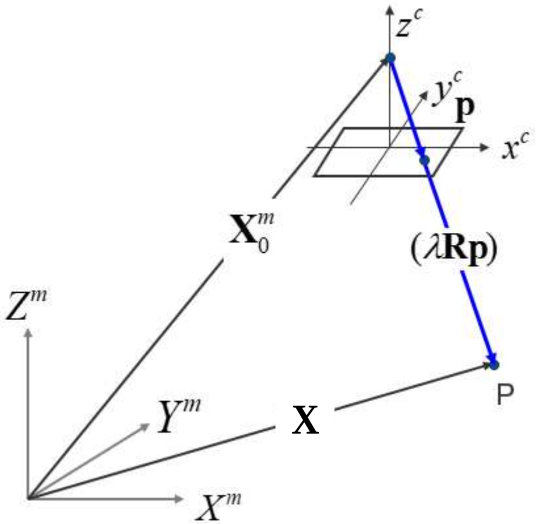

$$\mathbf{X} + \mathbf{v}_X = \mathbf{X}_0^m + \lambda \cdot \mathbf{R}_c^m(\omega, \varphi, \kappa) \cdot \mathbf{x}^c$$

- Collinearity equation

$$x + v_x = x_0 - c \cdot \frac{r_{11}(X - X_0^m) + r_{12}(Y - Y_0^m) + r_{13}(Z - Z_0^m)}{r_{31}(X - X_0^m) + r_{32}(Y - Y_0^m) + r_{33}(Z - Z_0^m)}$$

$$y + v_y = y_0 - c \cdot \frac{r_{21}(X - X_0^m) + r_{22}(Y - Y_0^m) + r_{23}(Z - Z_0^m)}{r_{31}(X - X_0^m) + r_{32}(Y - Y_0^m) + r_{33}(Z - Z_0^m)}$$

GNSS-supported AT

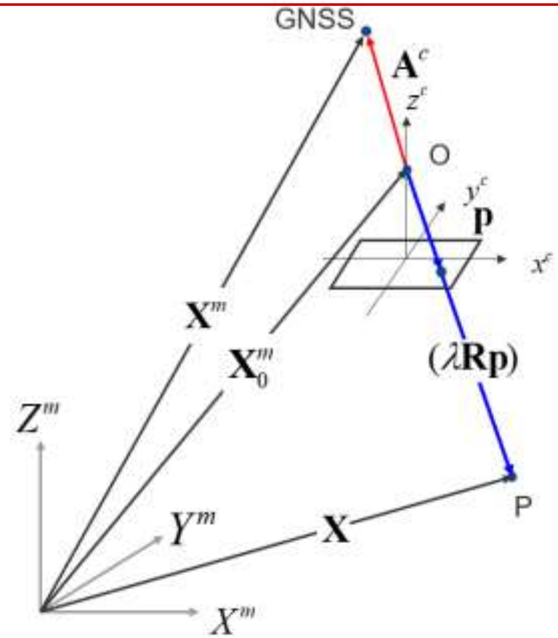

adding GNSS position

$$\mathbf{X}^m + \mathbf{v}_X^m = \mathbf{X}_0^m + \mathbf{R}_c^m(\omega,\varphi,\kappa)\cdot \mathbf{A}^c + \mathbf{S}^m$$

$$\mathbf{X} + \mathbf{v}_X = \mathbf{X}_0^m + \lambda \cdot \mathbf{R}_c^m(\omega,\varphi,\kappa)\cdot \mathbf{x}^c$$

- GNSS perspective centre coordinate observations significantly reduce requirements on geodetic measurements, i.e. ground control points
- Position observations are introduced as weighted observations
- System calibration (i.e. lever arm vector) is assumed to be known or determinable. Additional systematic GNSS shifts can be added to the model

GNSS/inertial-supported AT / Direct georeferencing

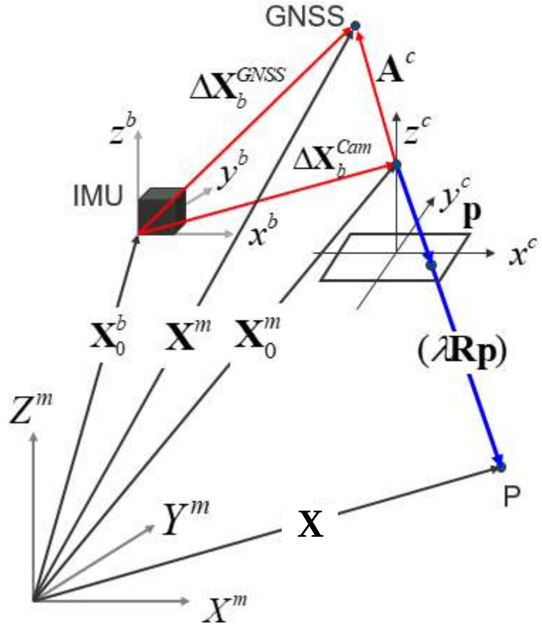

adding GNSS/inertial EO parameters

$$\mathbf{X}^m + \mathbf{v}_X^m = \mathbf{X}_0^m + \mathbf{R}_c^m(\omega,\varphi,\kappa)\cdot\mathbf{A}^c + \mathbf{S}^m$$

$$\mathbf{R}_b^m(\Phi + v_\Phi, \Theta + v_\Theta, \Psi + v_\Psi) = \mathbf{R}_c^m(\omega,\varphi,\kappa)\cdot\mathbf{R}_b^c(\Delta\omega,\Delta\varphi,\Delta\kappa)$$

$$\mathbf{X} + \mathbf{v}_X = \mathbf{X}_0^m + \lambda\cdot\mathbf{R}_c^m(\omega,\varphi,\kappa)\cdot\mathbf{x}^c$$

- GNSS / inertial orientation parameters are beneficial - especially for non-standard block configurations, reducing requirements on control and tie points
- EO direct observations are introduced as weighted observations
- But: System calibration (i.e. Boresight parameter) is assumed to be known or determinable

Study: High-precision 3D monitoring for engineering applications

Research project with BfG Koblenz, Testsite Ship-lock Hessigheim

Quelle: BAW, 2016

Testsite Ship-lock Hessigheim

(netto) Site extensions: 570 m (EW) x 780 m (NS)

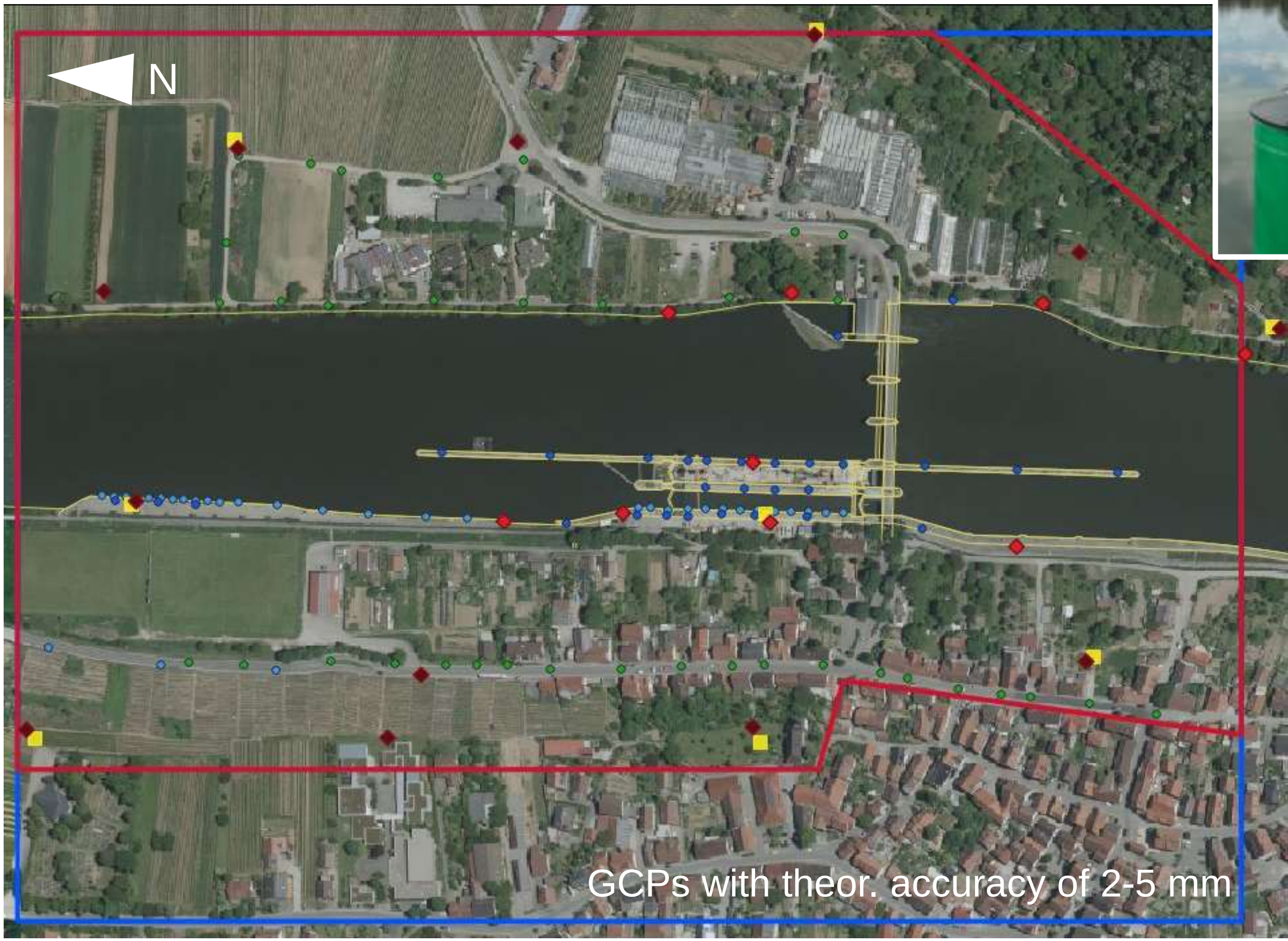

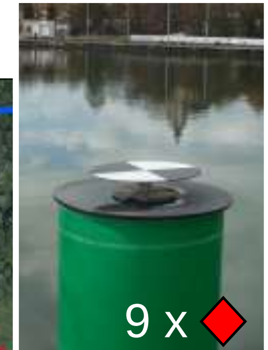

UAV – Systems: Photogrammetry and LiDAR

- *CopterSystems* with PhaseOne IXM 100, 35 mm lens (**fix-focussed** to 60m distance, **lab-calibrated**)
- Mean flying height: 40 m above ground
  Mean nom. **GSD: 4.0 mm**
  Image area coverage: ~50 x 35 m²
- Accuracy: scaleable (1 pix aspired)

- *Geografie Uni Innsbruck* RiCOPTER with VUX-1UAV
- Point density: 300-400 Pts/m² (per strip), 800 Pts/m² (multiple overlap)
  - 2 x Sony Alpha 6000 camera oblique
  - 1.2-2.0 cm GSD
- Accuracy: 10 mm, Precision: 5 mm

Testsite Ship-lock Hessigheim

Flightcampaign November 2018

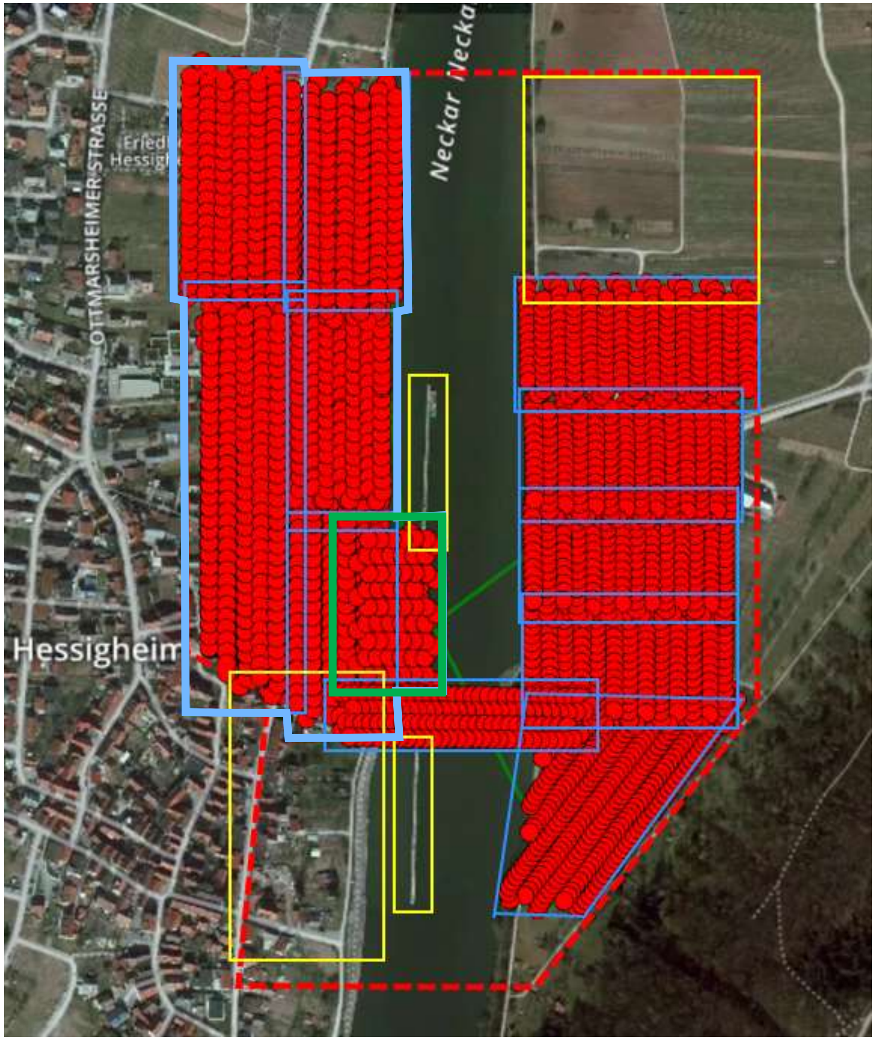

- PhaseOne IXM 100 data
  - 12(+2) flights @ 2 days
  - Calibration flight (cross pattern) at first day (ship lock)
  - Quite poor sunlight / weather as flights were done Nov 14/15 2018 – no full coverage of test site possible
- Calibration block
  - 148 images, 2 different flight heights (40m & 50m)
- Block Western-Shore
  - 1037 (909) Images, one flight height (40m)

Calibration block: Performance of GNSS/inertial EO

UAV-application of Applanix APX-15 EI UAV

Residuals at camera **positions** (observed – adjusted)

[10 cm]

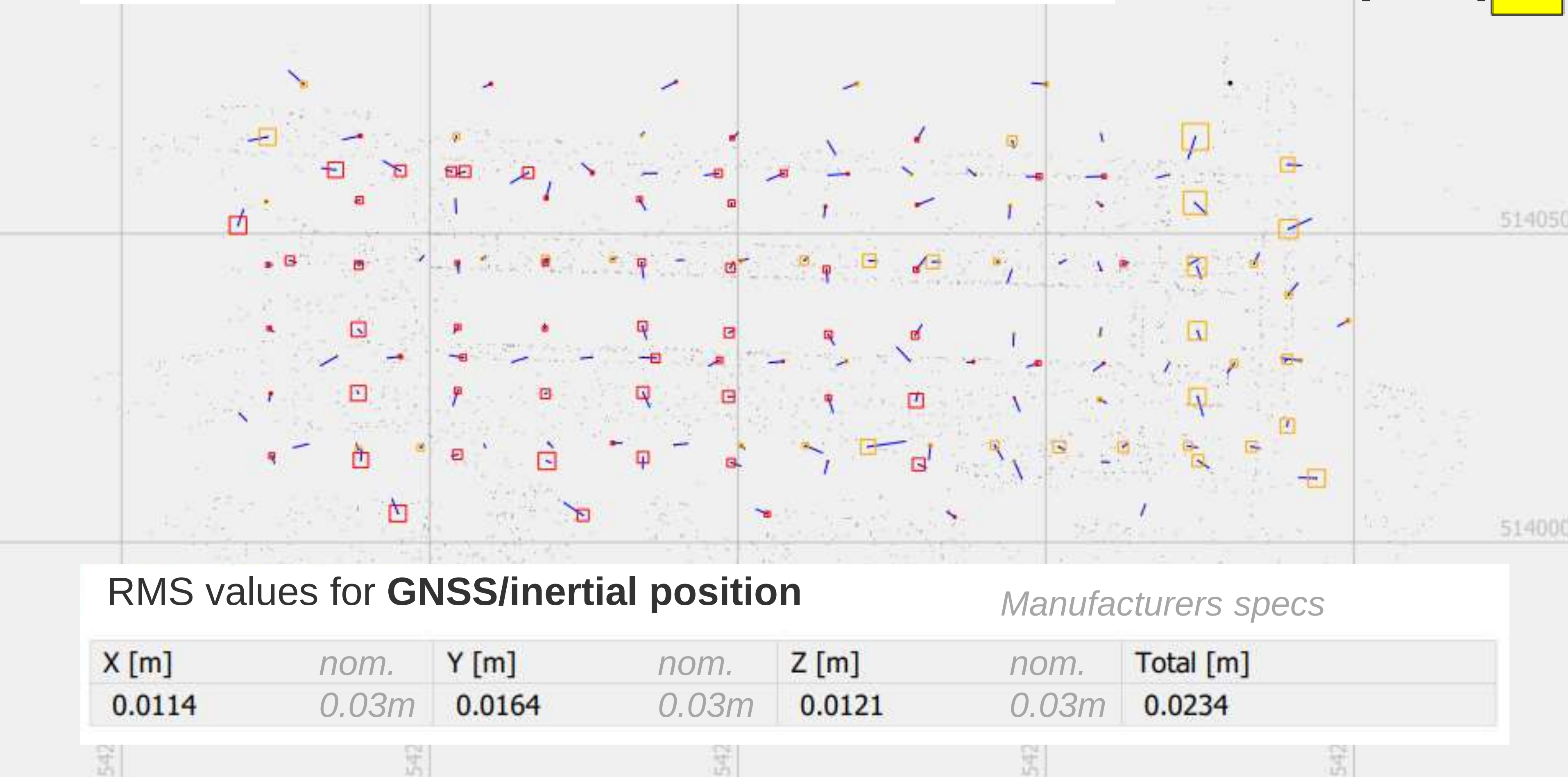

RMS values for **GNSS/inertial position**

Manufacturers specs

X [m]	*nom.*	Y [m]	*nom.*	Z [m]	*nom.*	Total [m]
0.0114	*0.03m*	0.0164	*0.03m*	0.0121	*0.03m*	0.0234

Calibration block: Performance of GNSS/inertial EO

UAV-application of Applanix APX-15 EI UAV

Residuals at camera **attitude** (observed – adjusted)

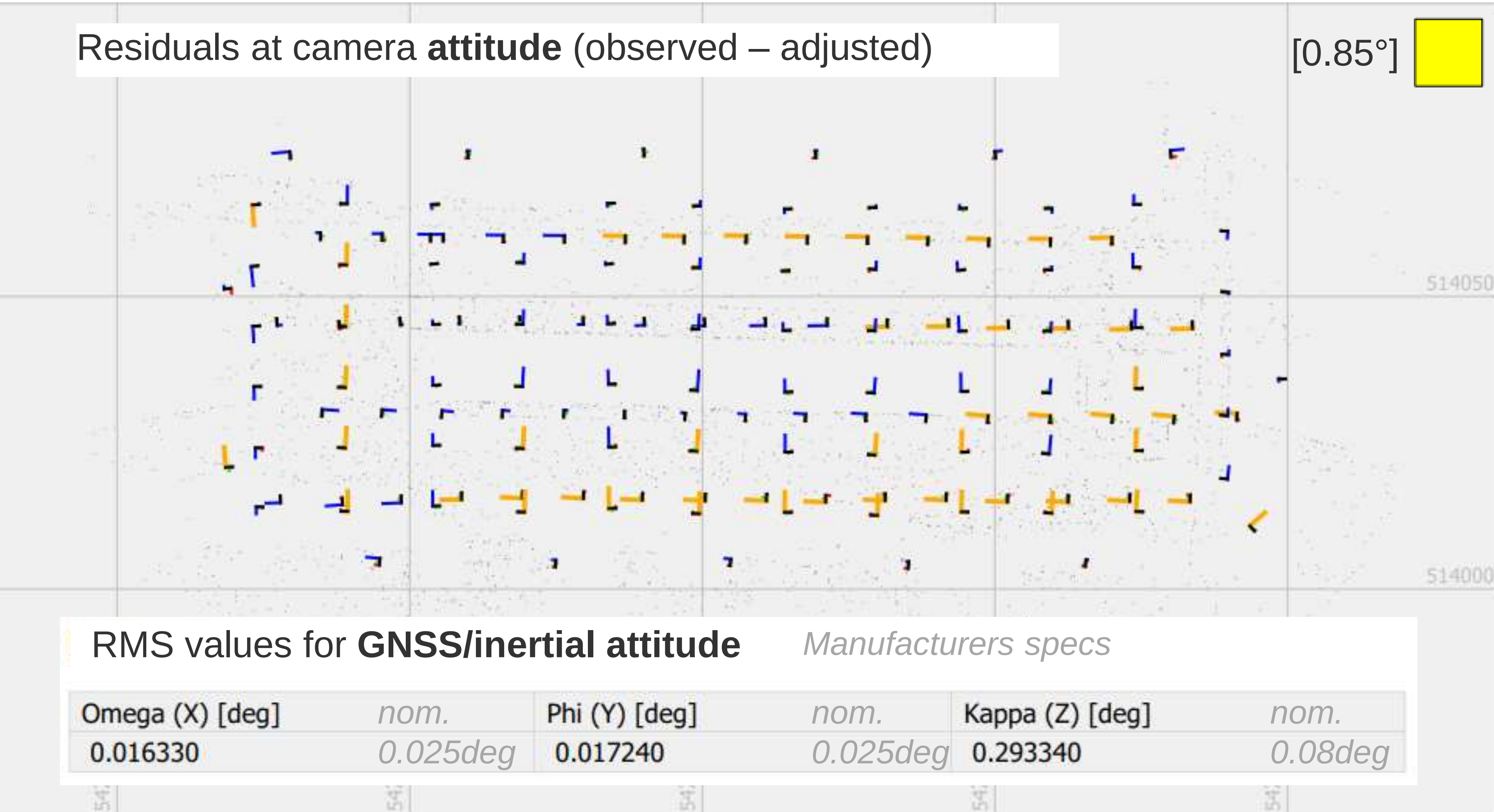

RMS values for **GNSS/inertial attitude** *Manufacturers specs*

Omega (X) [deg]	*nom.*	Phi (Y) [deg]	*nom.*	Kappa (Z) [deg]	*nom.*
0.016330	*0.025deg*	0.017240	*0.025deg*	0.293340	*0.08deg*

Calibration block: cross-pattern / ship-lock

Impact of GNSS- and GNSS/inertial-data in AT

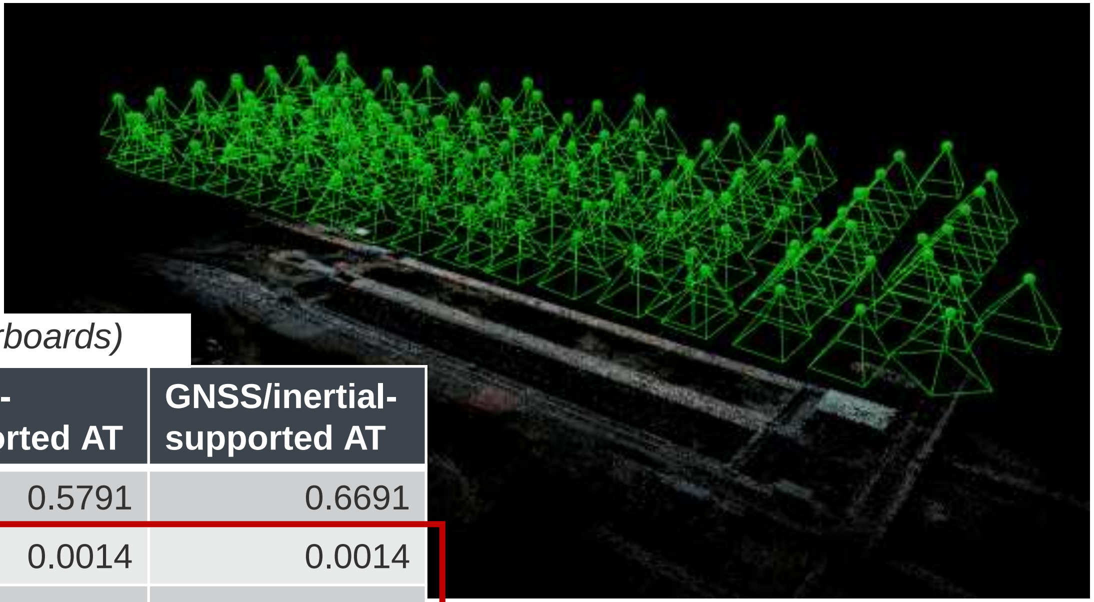

Residuals from 20 Checkpoints (Checkerboards)

		AT with GCPs only	GNSS-supported AT	GNSS/inertial-supported AT
Sigma0 [pix]		0.5815	0.5791	0.6691
RMS	X [m]	0.0016	0.0014	0.0014
	Y [m]	0.0021	0.0023	0.0022
	Z [m]	0.0042	0.0019	0.0018
STD	X [m]	0.0016	0.0014	0.0014
	Y [m]	0.0021	0.0021	0.0022
	Z [m]	0.0038	0.0019	0.0017
Max.	X [m]	-0.0030	-0.0026	0.0033
	Y [m]	-0.0062	-0.0067	-0.0056
	Z [m]	0.0110	-0.0035	0.0034

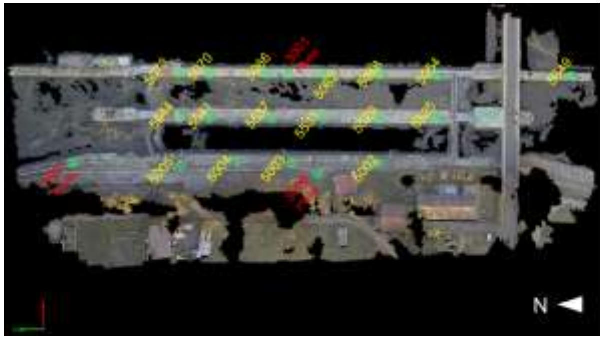

3 GCPs (Pillars)
20 CHPs

Calibration block: cross-pattern / ship-lock

Impact of GNSS- and GNSS/inertial data in AT

AT with GCPs only

GNSS-supported AT

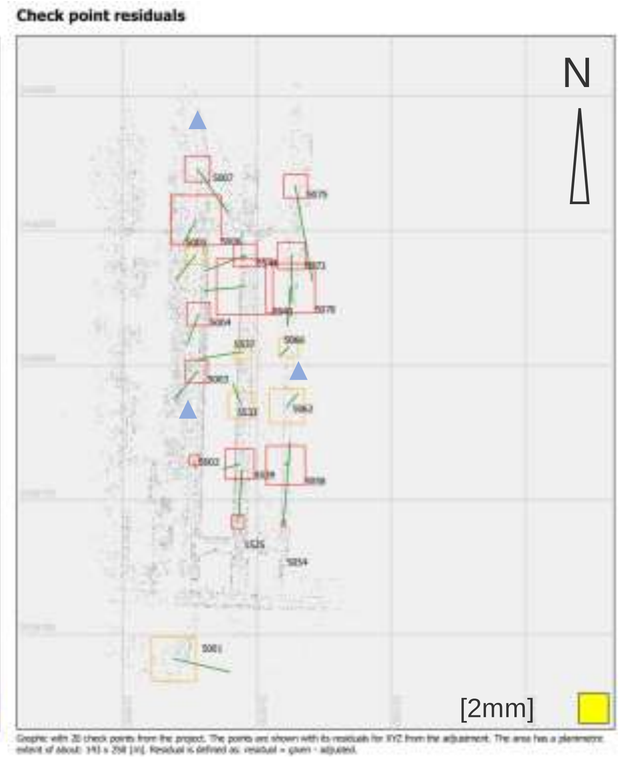

GNSS/inertial-supported AT

3 GCPs (Pillars)
20 CHPs

Block Western-Shore

Impact of GNSS- and GNSS/inertial data in AT

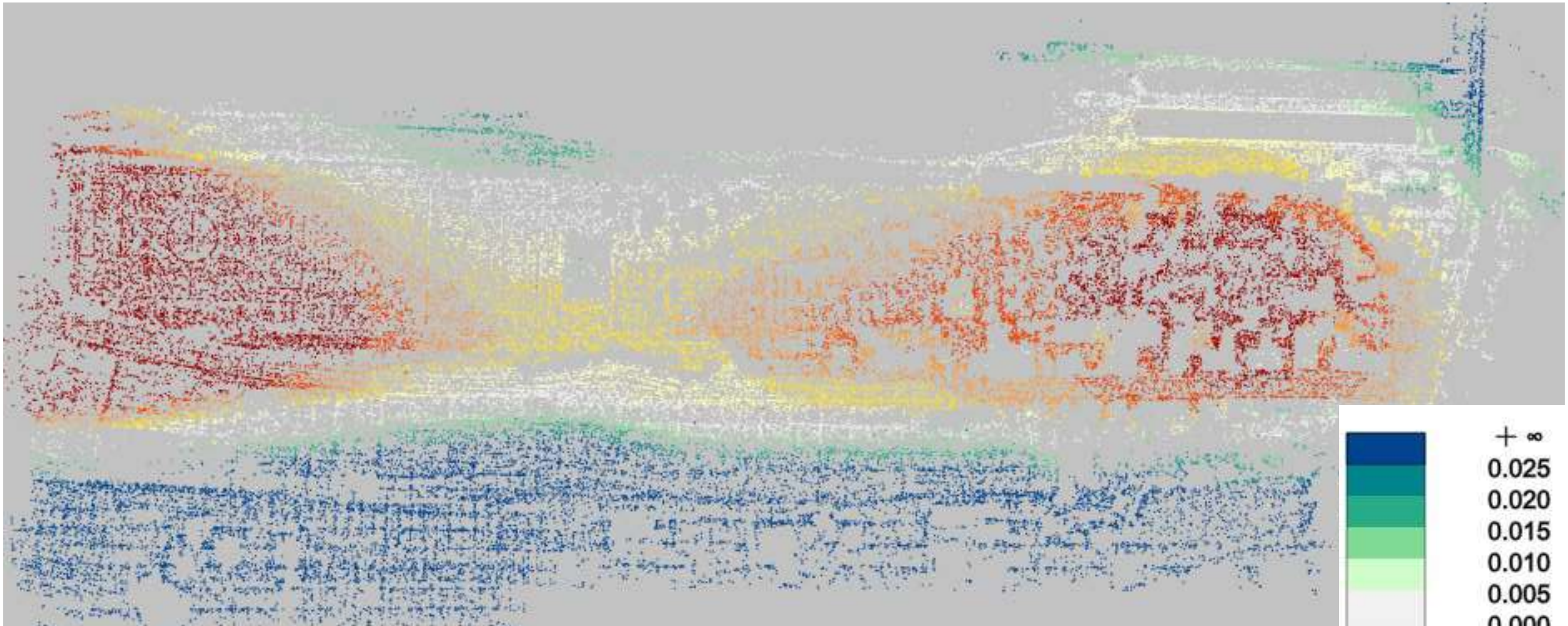

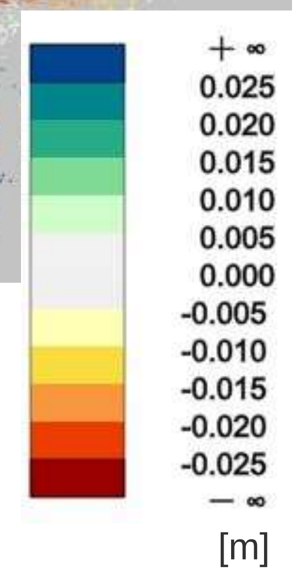

Comparison 3D object points ΔZ (sparse point cloud after AT)

GCP only based AT versus **GNSS-supported** AT

Block Western-Shore

Impact of GNSS- and GNSS/inertial data in AT

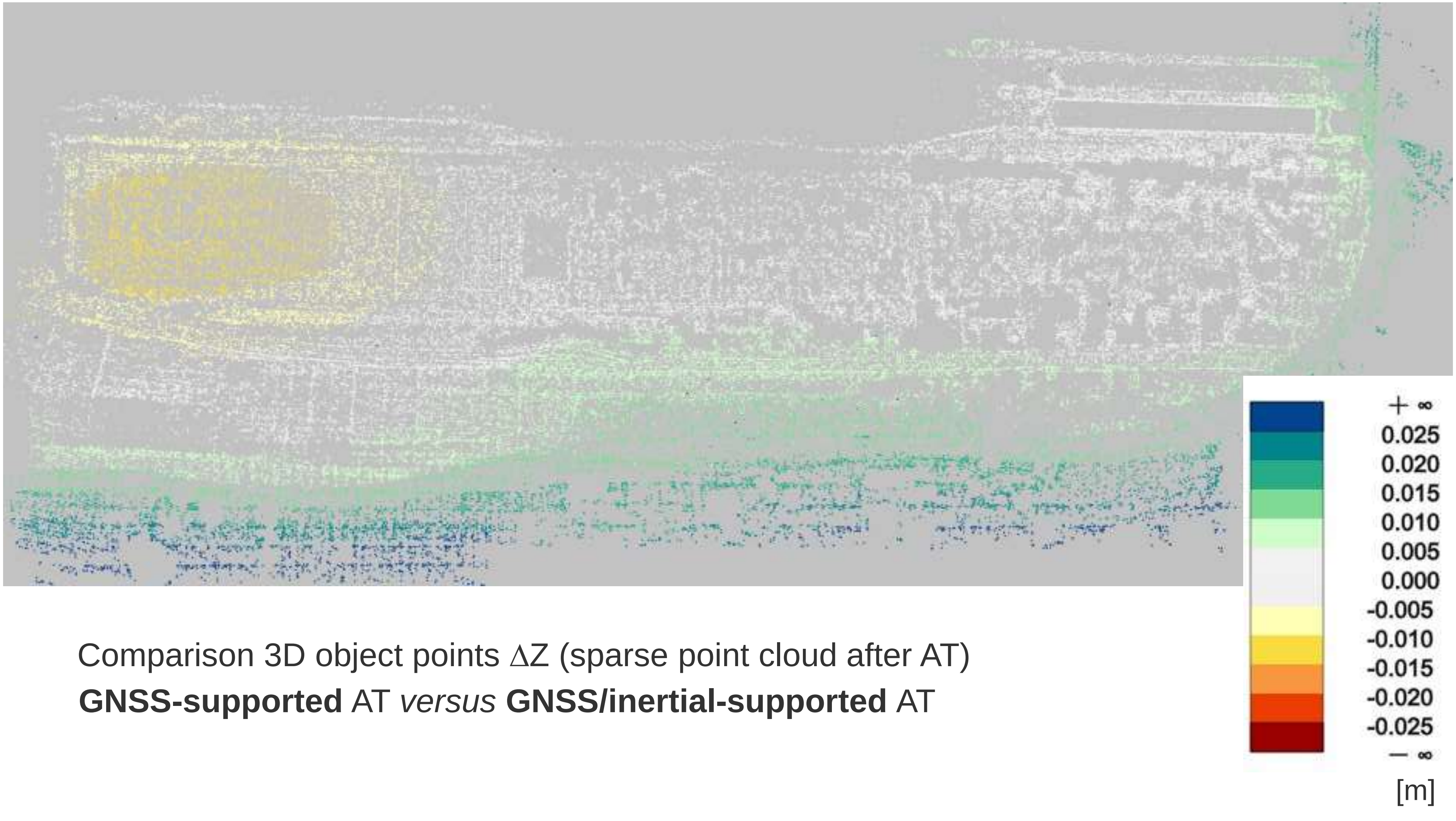

Comparison 3D object points ΔZ (sparse point cloud after AT)

GNSS-supported AT *versus* **GNSS/inertial-supported** AT

Questions & Comments ?!

- Is UAV-based mapping so much different to regular flight campaigns?

- “With a little help from my friends” – using GNSS/inertial-based georeferencing for UAV-imagery – case study

- Are there further updates in the georeferencing of UAV-based imagery?
  - Extended AT with **relative position and attitude** control
  - **Fast** AT
  - **Hybrid** LiDAR & images georeferencing
  - **Tightly coupling** of GNSS/inertial data & image observations in one adjustment

Universität Stuttgart

DGPF

State-of-the-art in UAV-based mapping – an update

Are there any further updates in georeferencing of UAV-based imagery?

ifp

Direct Georeferencing / Integr. sensor orientation

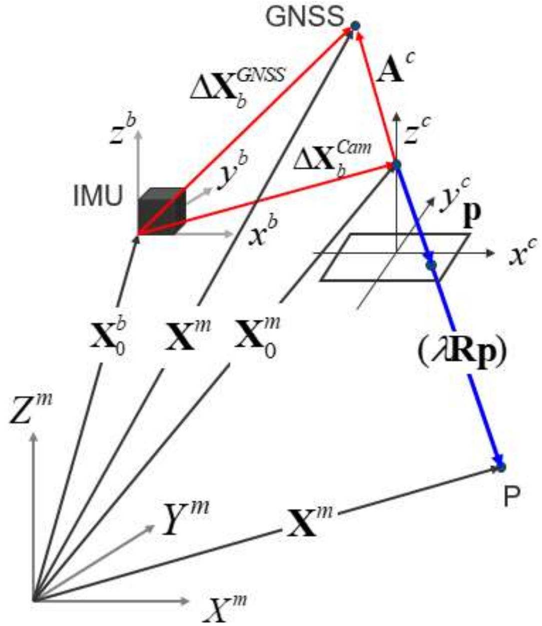

absolut GNSS/inertial EO elements

$$\mathbf{X}^m + \mathbf{v}_X^m = \mathbf{X}_0^m + \mathbf{R}_c^m(\omega,\varphi,\kappa)\cdot\mathbf{A}^c + \mathbf{S}^m$$

$$\mathbf{R}_b^m(\Phi + v_\Phi, \Theta + v_\Theta, \Psi + v_\Psi) = \mathbf{R}_c^m(\omega,\varphi,\kappa)\cdot\mathbf{R}_b^c(\Delta\omega,\Delta\varphi,\Delta\kappa)$$

- GNSS / inertial orientation parameters are **beneficial** - especially for such corridor flights, reducing requirements on link points (and points)
- **But**: System calibration (generally Boresight parameter) is assumed to be known or determinable
- **Problem**: **corridor only provides poor geometry**, in addition camera might no be really **stable** over time

GNSS/inertial supported AT
using relative GNSS/inertial EO parameters

Why using **relative** GNSS/inertial EO params / relative aerial control?

- **elimination of system calibration parameters**;
- stationary time dependent stochastic model for relative aerial control;
- new photogrammetric observation models for horizontal map-projected coordinates;
- new attitude aerial control observation models to avoid re-parameterisations steps

M. Blázquez & I. Colomina (2012): Relative INS/GNSS aerial control in integrated sensor orientation: Models and performance, in ISPRS Journal of Photogrammetry and Remote Sensing 67 (2012) 120–133 http://doi.org/10.1016/j.isprsjprs.2011.11.003

AT using relative aerial control

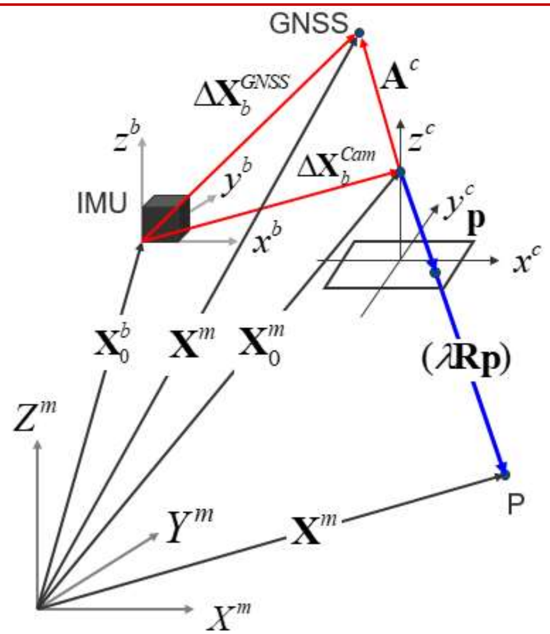

absolut GNSS/inertial EO elements

$$\mathbf{X}^m + \mathbf{v}_X^m = \mathbf{X}_0^m + \mathbf{R}_c^m(\omega,\varphi,\kappa)\cdot\mathbf{A}^c + \mathbf{S}^m$$

$$\mathbf{R}_b^m(\Phi + v_\Phi, \Theta + v_\Theta, \Psi + v_\Psi) = \mathbf{R}_c^m(\omega,\varphi,\kappa)\cdot\mathbf{R}_b^c(\Delta\omega,\Delta\varphi,\Delta\kappa)$$

- AT using **relative** GNSS/inertial aerial control exterior orientation elements
  - ▶ Boresight-Alignment $\mathbf{R}_b^c(\Delta\omega,\Delta\varphi,\Delta\kappa)$ is eliminated

$$\Delta\mathbf{X}^m(t_{ij}) + \mathbf{v}_{\Delta X}^m = \left(\mathbf{X}_0^m(t_j) - \mathbf{X}_0^m(t_i)\right) + \left(\mathbf{R}_c^m(\omega_{t_j},\varphi_{t_j},\kappa_{t_j}) - \mathbf{R}_c^m(\omega_{t_i},\varphi_{t_i},\kappa_{t_i})\right)\cdot\mathbf{A}^c$$

$$\Delta\mathbf{R}_b^m(\Phi_{t_{ij}} + v_\Phi, \Theta_{t_{ij}} + v_\Theta, \Psi_{t_{ij}} + v_\Psi) = \mathbf{R}_c^m(\omega_{t_j},\varphi_{t_j},\kappa_{t_j})\cdot\mathbf{R}_m^c(\omega_{t_i},\varphi_{t_i},\kappa_{t_i})$$

AT with relative GNSS/inertial aerial control

Position

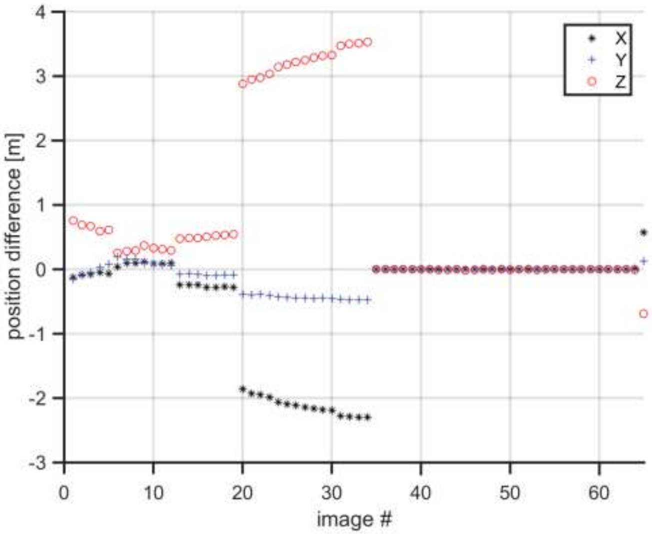

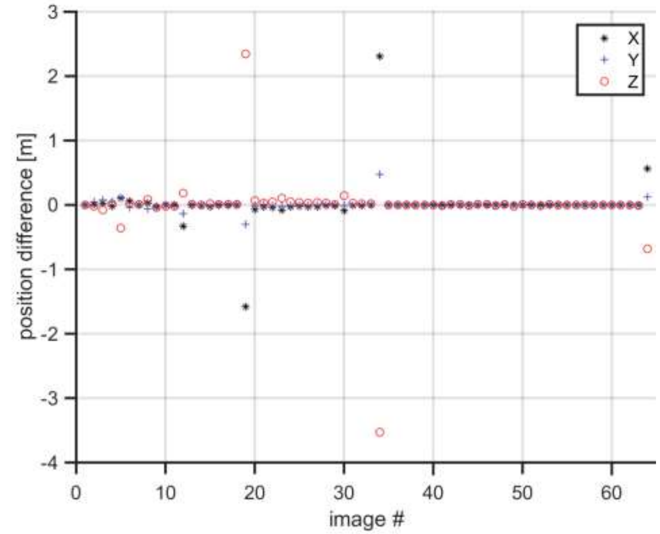

Attitude

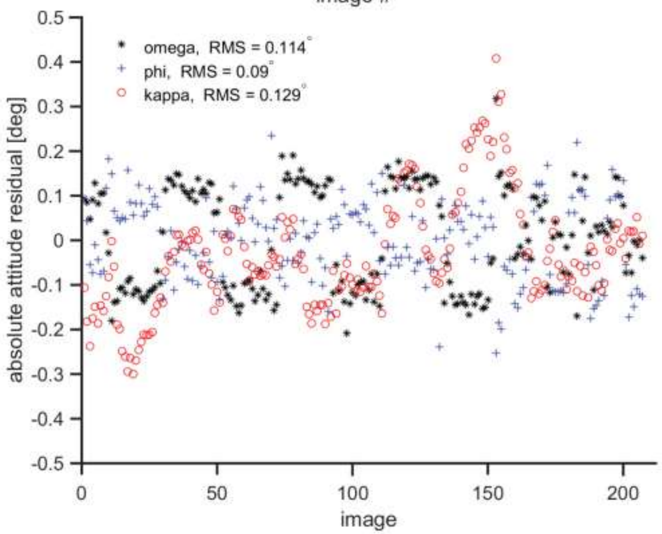

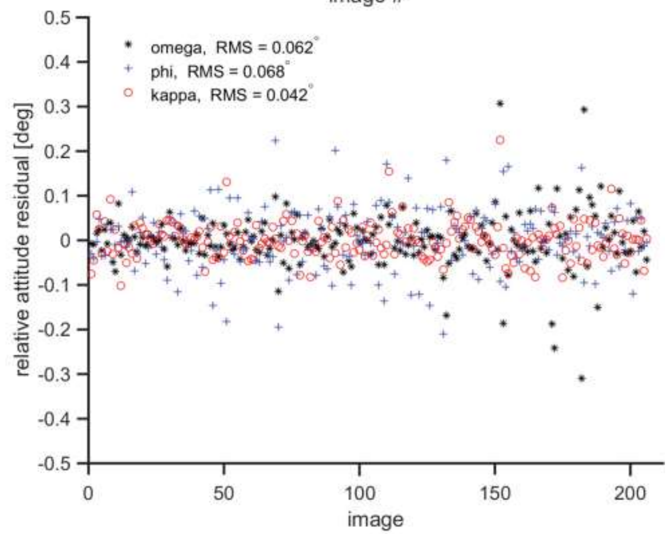

absolute

relative

AT with relative GNSS/inertial aerial control

Influence of GNSS receiver quality (positioning only)

Position differences
JAVAD-ublox

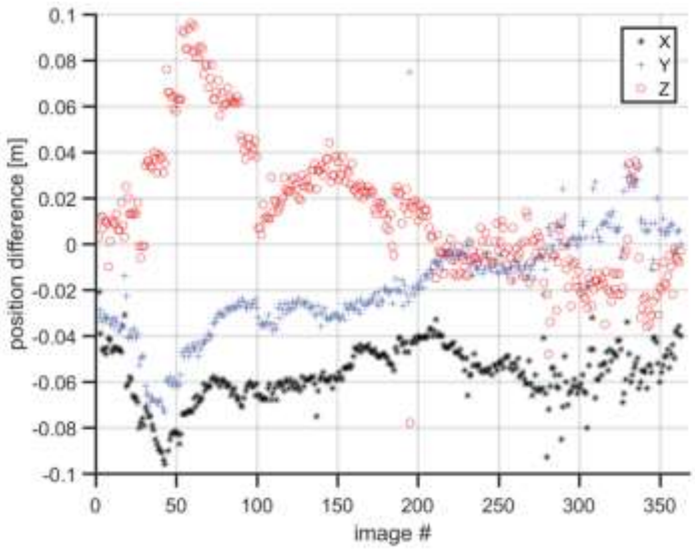

absolut

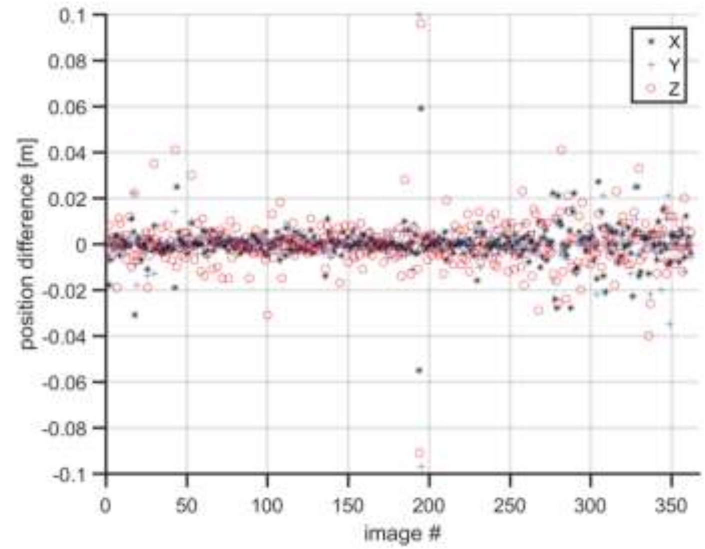

relativ

Javad OEM TR-G3T

216 channels each of GPS L1/L2/L2C/L5, GLONASS L1/L2, Galileo E1/E5A

Costs: ~10000 $US

ublox NEO-8T

72-channel u-blox GPS/QZSS L1 C/A, GLONASS L10F, BeiDou B1

Costs: ~75 $US

Fast AT

- particular case of Integrated Sensor Orientation (GNSS/inertial supported AT) characterized by the use of the following observations:
  - (time) position and attitude (tPA) **aerial control observations**, either in the absolute or relative mode, for all images.
  - Ground control point observations for a **limited number (in principle) of points** and images.
  - Image coordinate observations **for the ground control points only**.

M. Blázquez & I. Colomina (2012): Fast AT: A simple procedure for quasi direct orientation, in ISPRS Journal of Photogrammetry and Remote Sensing 71 (2012) 1–11
https://doi.org/10.1016/j.isprsjprs.2012.04.005

Fast AT
Conceptual Layout (1/2)

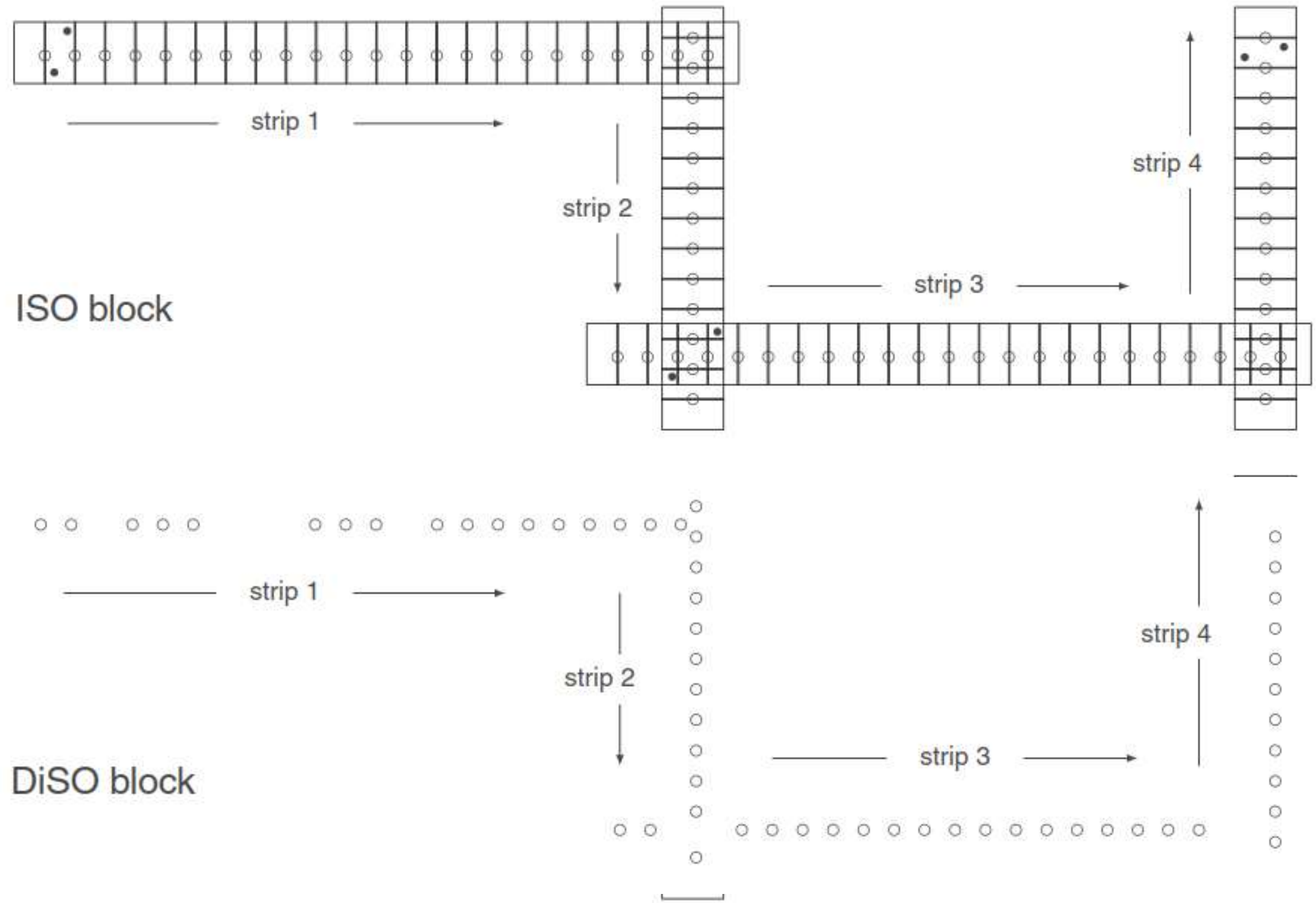

Fast AT
Conceptual Layout (2/2)

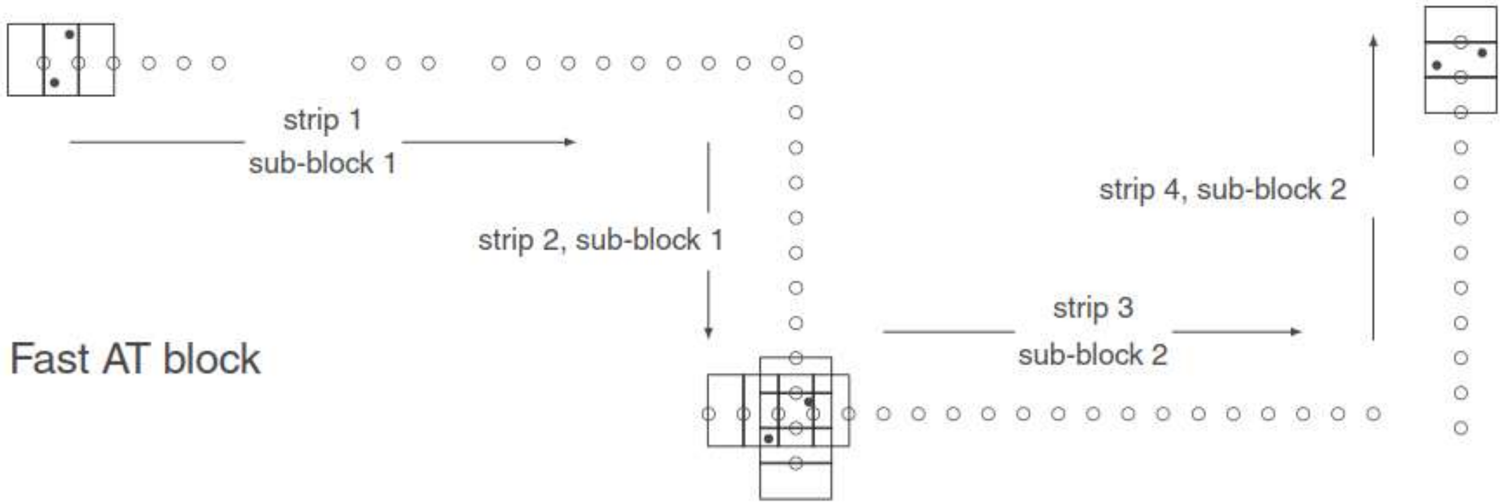

○ image and tPA aerial control point

• ground control point (GCP)

☐ image with one or more photo-measurements

ISO block:	23 + 13 + 23 + 13 images, photo-measurements in all images.
Fast AT block:	18 + 13 + 20 + 12 images, photo-measurements in 2 + 3 + 3 + 2 images, 2 sub-blocks, no need for image/strip overlap, image overlap recommended in areas with GCPs.
DiSO block:	17 + 12 + 18 + 11 images, no photo-measurements, no GCPs, no overlap requirements.

Fast AT

InSO – indirect sensor orientation
ISO – integrated sensor orientation
DiSO – direct sensor orientation

Observations of InSO, ISO, Fast AT and DiSO.

Observations	InSO	ISO	Fast AT	DiSO
tPA/tPVA aerial control	NO	YES	YES	YES
Ground control points	YES	YES	YES	NO
	many	few	few	
Image coordinates	YES	YES	YES	NO
	many	many	few	

Properties of ISO, Fast AT and DiSO.

Properties	ISO	Fast AT	DiSO
Precision	+	0	0
Accuracy	+	0	–
Reliability	+	0	–
Cost	+	0	–
Time	+	0	–

+: high. 0: average. –: low.

Fast AT
potential applications

- Fast AT is of interest in situations where ISO (integrated sensor orientation) is not feasible or required and where DiSO (direct sensor orientation) is not accurate or reliable enough. For instance, it may be used for ill-textured areas where image matching is difficult.
- for applications currently relying on DiSO, where accuracy and reliability matter, and that, for some reason, cannot afford the time and/or cost required by ISO and where the measurement or use of existing GCPs makes sense in the context of the application.
- can be used in combination with standard ISO procedures: **One possibility is that a small ISO block be used for camera calibration and that Fast AT be applied for larger blocks. The data acquisition for the ISO block can take place at any time, before, in between or after the Fast AT blocks are acquired. Sensor calibration parameters can then be computed and, later on, used as constants or observations in the Fast AT blocks.**

Fast AT
Mathematical Model

- Fast AT concept is independent from the particular functional models of the observation equations for image coordinate, ground control and aerial control observations
- Both possibilities
  - Classical use of EOP observations: classical use of tPA aerial control observations in absolute mode, **absolute Fast AT**
  - Relative use of EOP observations: use of tPA aerial control observations in relative mode, **relative Fast AT**

Influence of Aerial Control on Mapping Accuracy Block Scenario

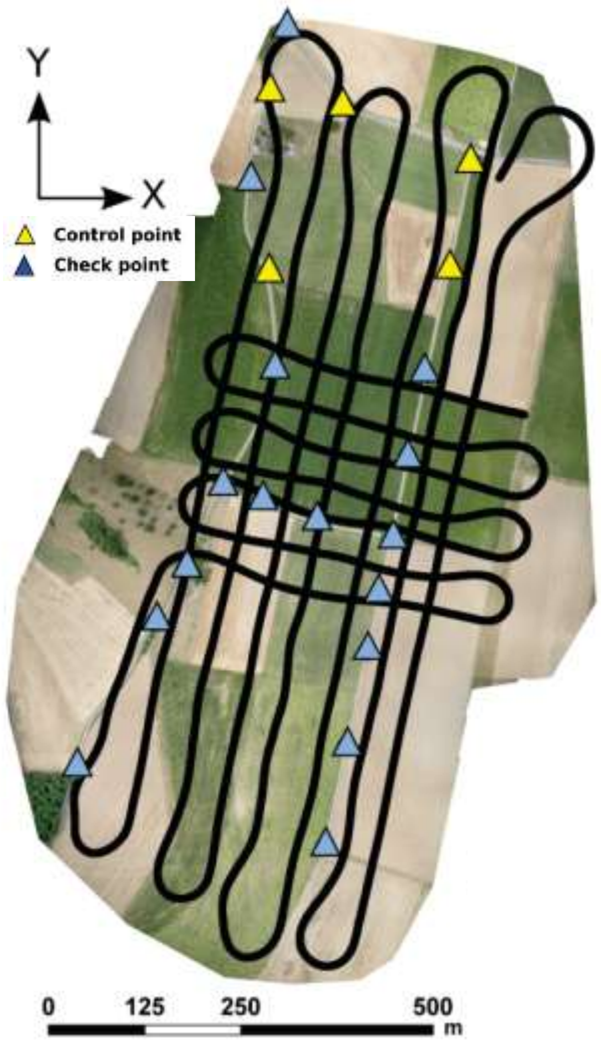

© Rehak, 2017

UAV test scenario

fixed-wing UAV with Sony NEX-5R,
GSD 4.5cm, 7 + 7 flight lines,
207 images, 80% / 60% overlap
20 GCP / ChP (notice distribution!)

Test scenarios

Mode	Position cont.	Attitude cont.	Camera cal.	Boresight
Indirect SO	-	-	Yes	-
ISO	Absolute	Absolute	Yes	Known
ISO	Absolute	Relative	Yes	-
ISO	Relative	Relative	Yes	-
Fast AT	Absolute	Absolute	No	Known
Fast AT	Absolute	Relative	No	-
Fast AT	Relative	Relative	No	-
DiSO	Absolute	Absolute	No	Known

Influence of Aerial Control on Mapping Accuracy
Block Scenario

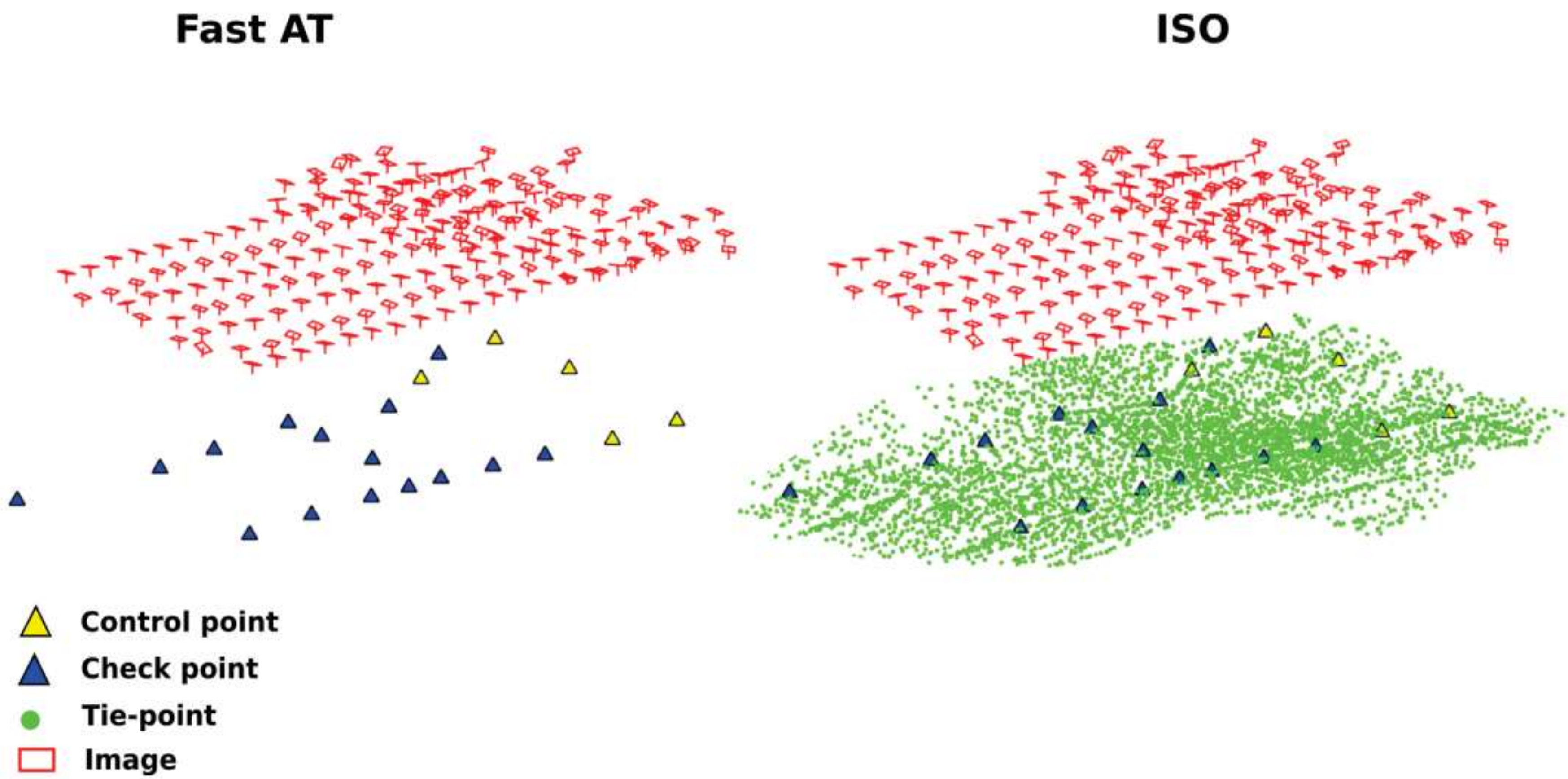

Distribution of GCPs, ChPs, and tie-points

UAV test using GNSS/inertial aerial control

Test	Mean [cm] X	Mean [cm] Y	Mean [cm] Z	RMS [cm] / [pix] X	RMS [cm] / [pix] Y	RMS [cm] / [pix] Z
Indirect Georeferencing (5 GCP / 15 ChP) with CamCal	6.8	0.8	-66.4	1.6 0.4	14.5 3.2	117.1 26.0
Direct Georeferencing (0 GCP / 20 ChP) with Boresight, no CamCal	-0.5	-1.3	-1.5	5.2 1.2	6.3 1.4	16.6 3.7
Integrated SO + abs. Position + abs. Attitude (5 GCP / 15 ChP) with Boresight & CamCal	0.6	1.6	3.5	3.2 0.7	2.9 0.6	5.3 1.2
Integrated SO + abs. Position + rel. Attitude (5 GCP / 15 ChP) no Boresight, with CamCal	-0.5	1.6	3.2	3.0 0.7	2.8 0.6	5.3 1.2
Fast AT + abs. Position + rel. Attitude (5 GCP / 15 ChP) no Boresight, no CamCal	0.8	3.8	-2.2	2.4 0.5	4.7 1.0	6.1 1.4

GSD: 4.5 cm

Hybrid LiDAR & image sensor orientation

Hybrid sensors

Standard georeferencing approach:

- each data stream processed / georeferenced independently, i.e.
  - LiDAR strip adjustment
  - Photogrammetric bundle
- Sensors moved on the same trajectory **not** considered!

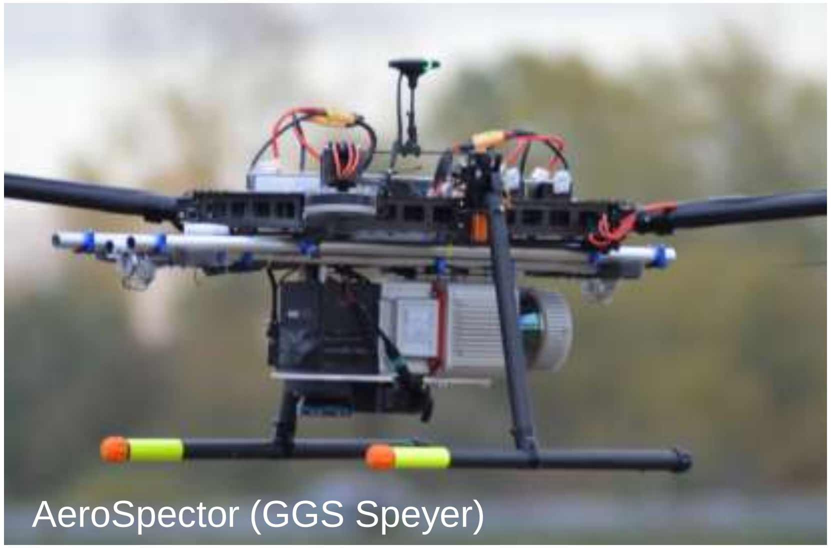

Hybrid LiDAR & image sensor orientation

- **simultaneously optimization** of the relative orientation and absolute orientation (georeference) of the lidar and image data.
- sensor orientations are optimized by **minimizing the discrepancies**
  (1) within the **overlap area** of flight strips and/or images and
  (2) with respect to **ground truth** if available
- rigorous modelling using the original measurements of the sensors (i.e. scanner: polar measurements, camera: image coordinates) and the flight trajectory of the aircraft

Glira, P., Pfeifer, N., and Mandlburger, G.: HYBRID ORIENTATION OF AIRBORNE LIDAR POINT CLOUDS AND AERIAL IMAGES, ISPRS Ann. Photogramm. Remote Sens. Spatial Inf. Sci., IV-2/W5, 567-574, https://doi.org/10.5194/isprs-annals-IV-2-W5-567-2019, 2019.

Hybrid LiDAR & image sensor orientation

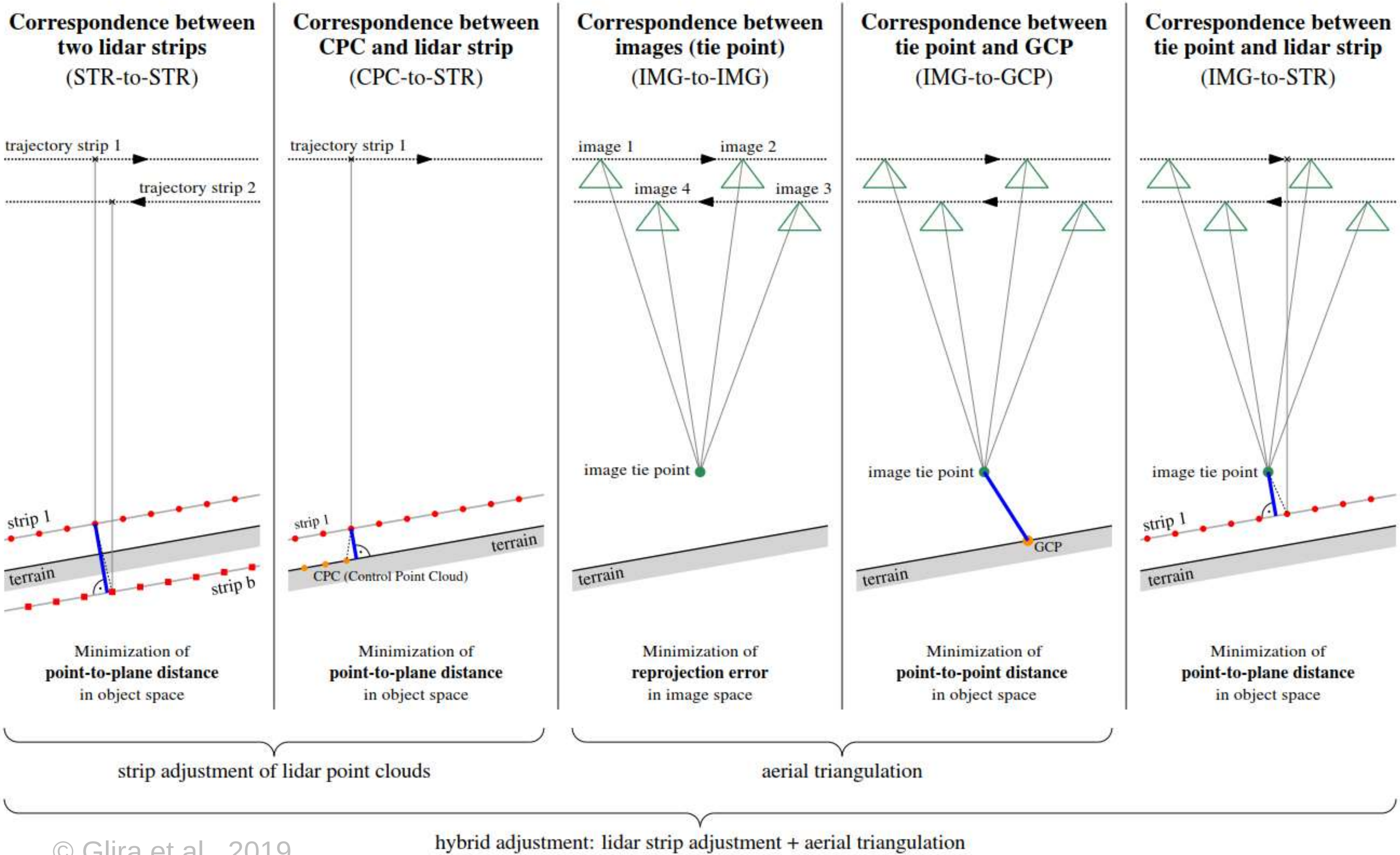

© Glira et al., 2019

Hybrid LiDAR & image sensor orientation

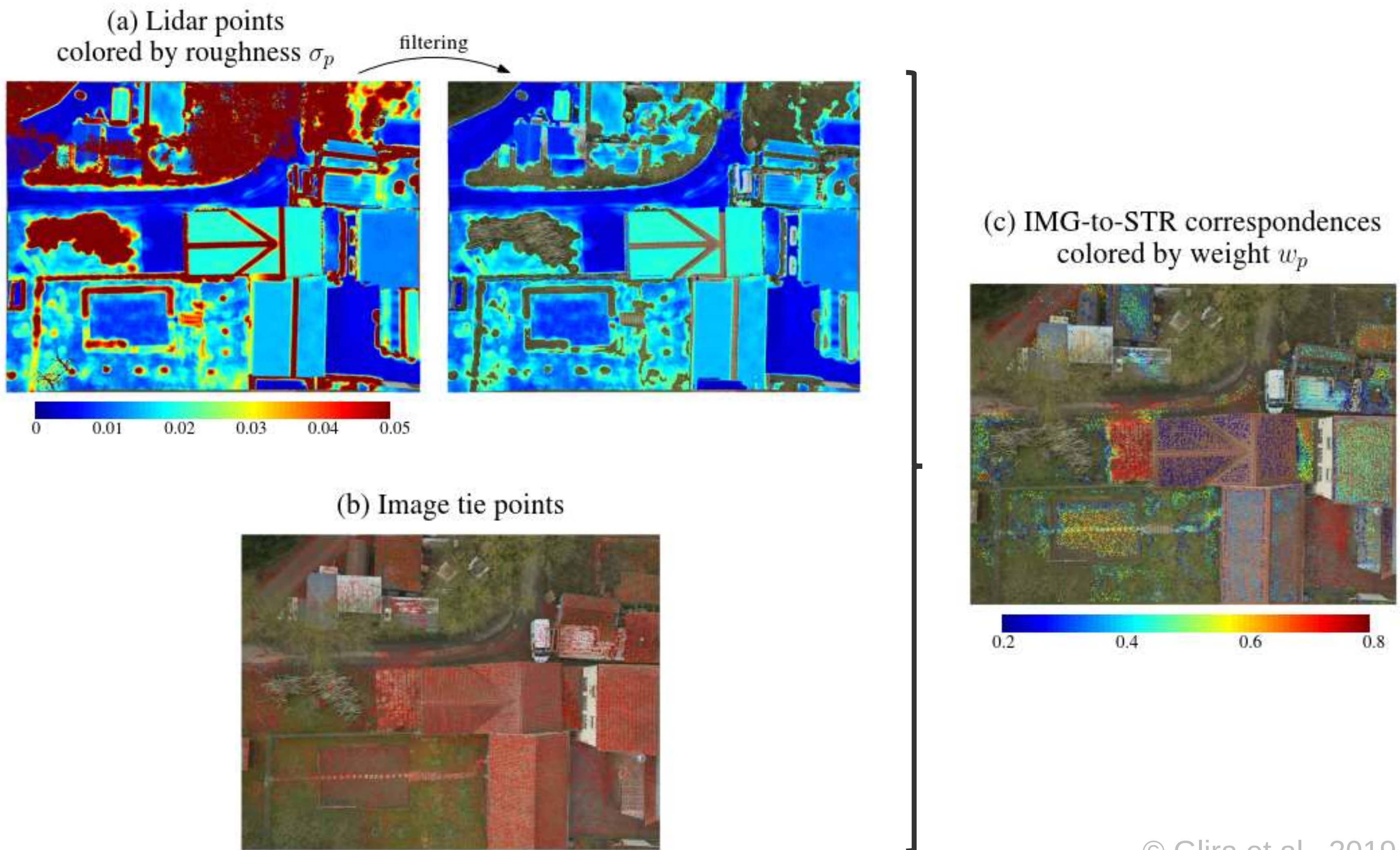

Hybrid LiDAR & image sensor orientation

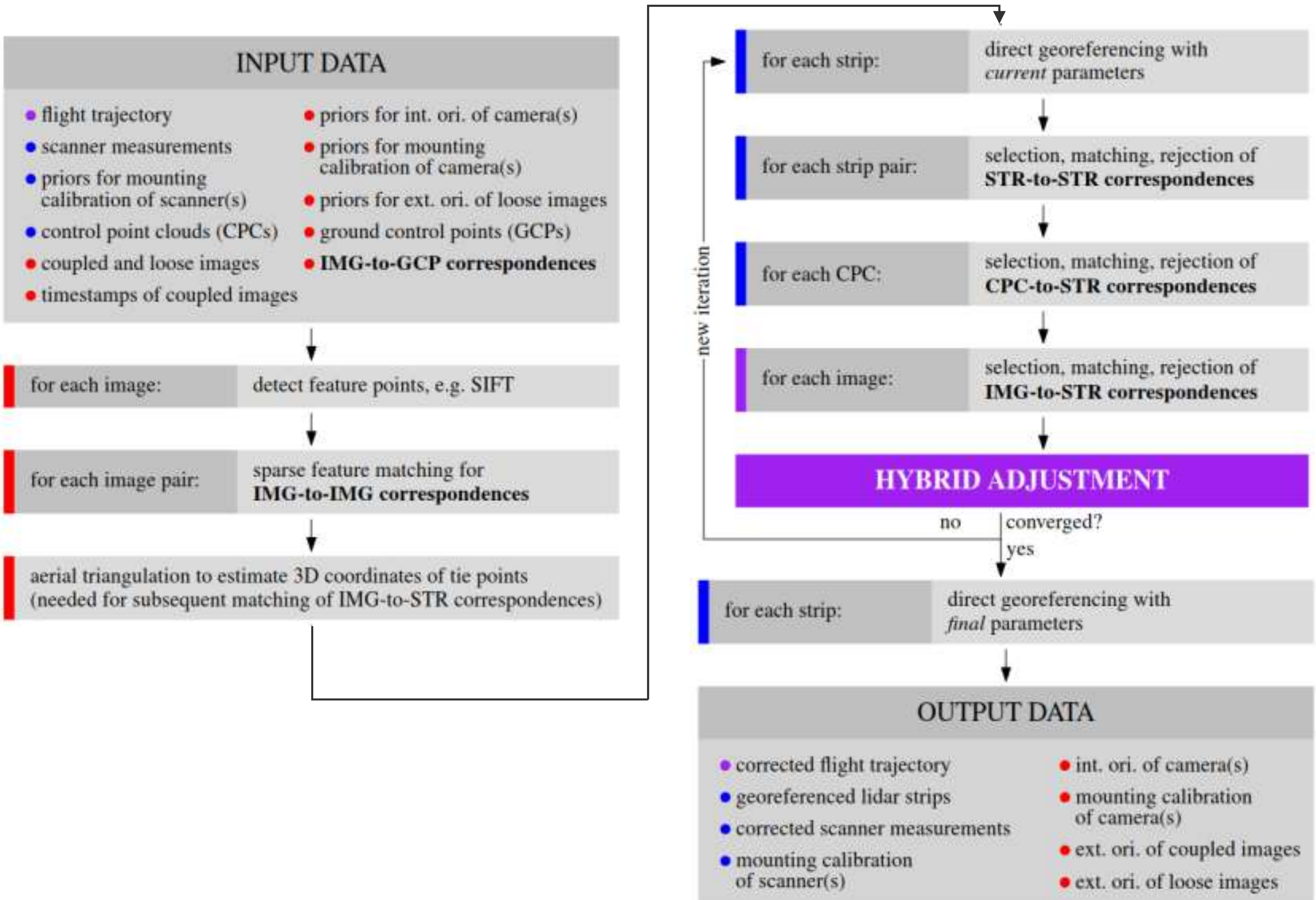

Stand-alone LiDAR processing

Flight campaign November 2018

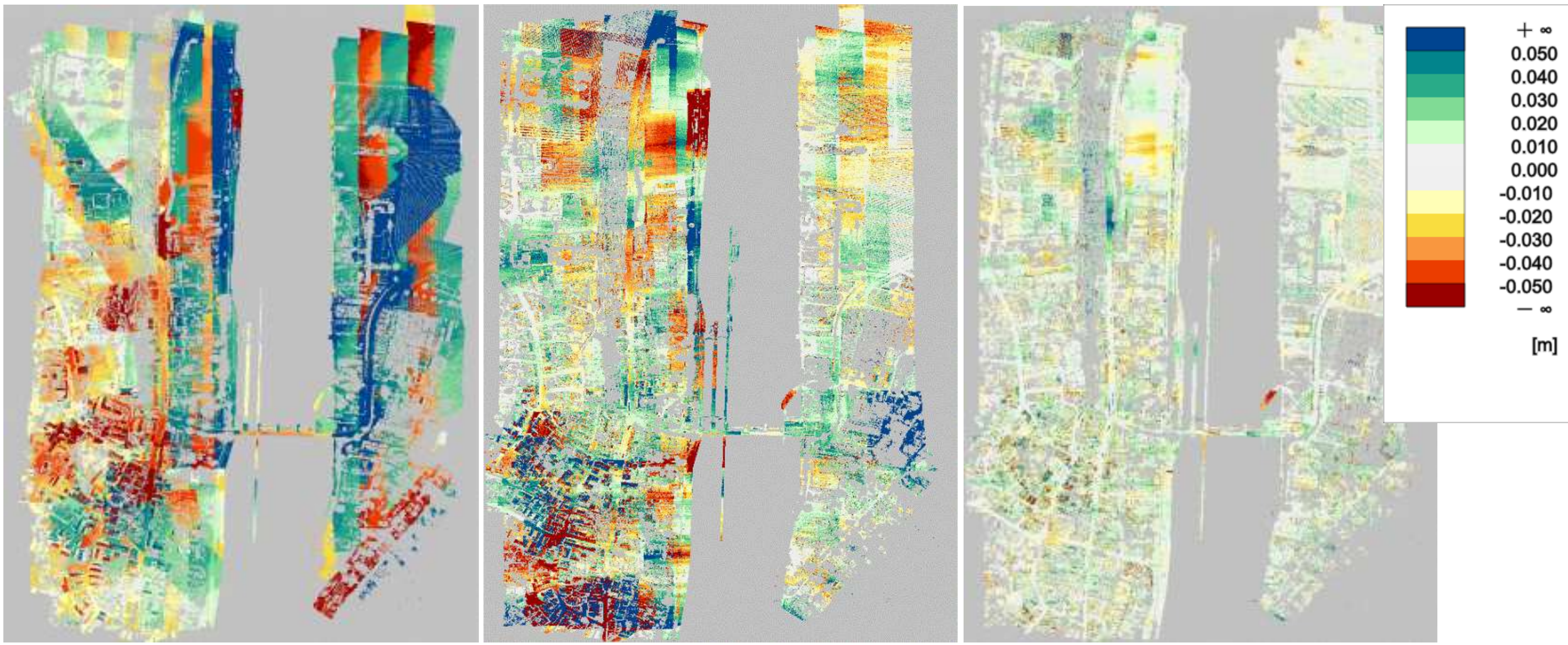

before strip-adjustment

After strip-adjustment, **bias** correction

After strip-adjustment, **spline model** correction

Stand-alone LiDAR processing

Absolute vertical accuracy from levelled (check-)planes

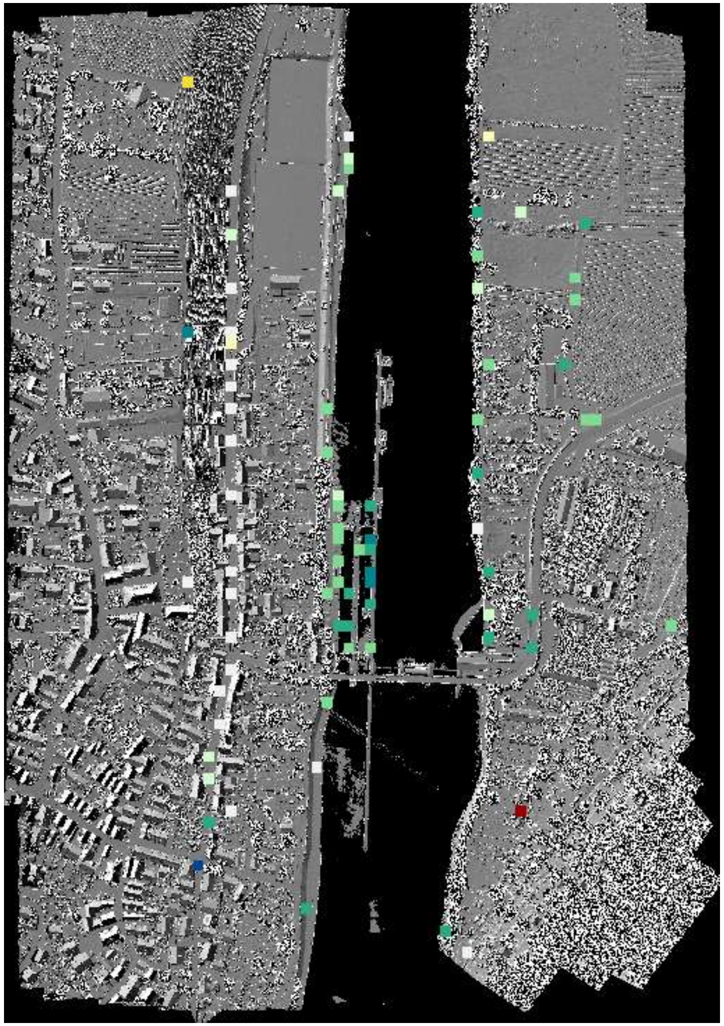

Bias model

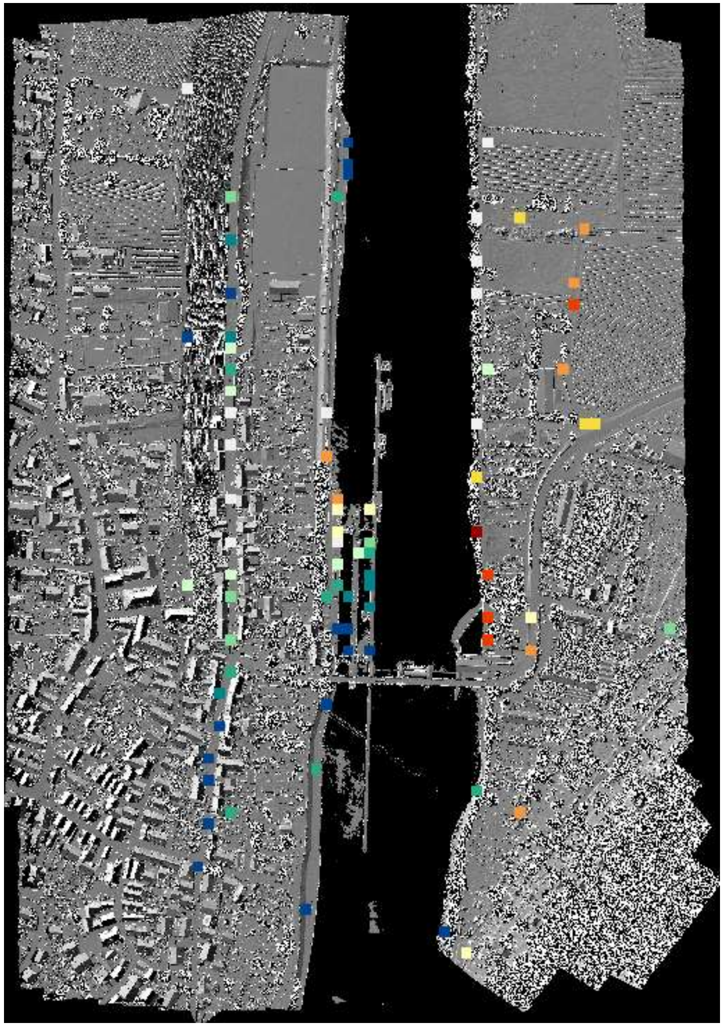

Spline model

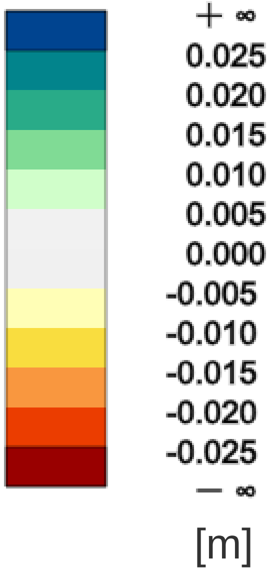

Stand-alone vs. hybrid LiDAR – image adjustment

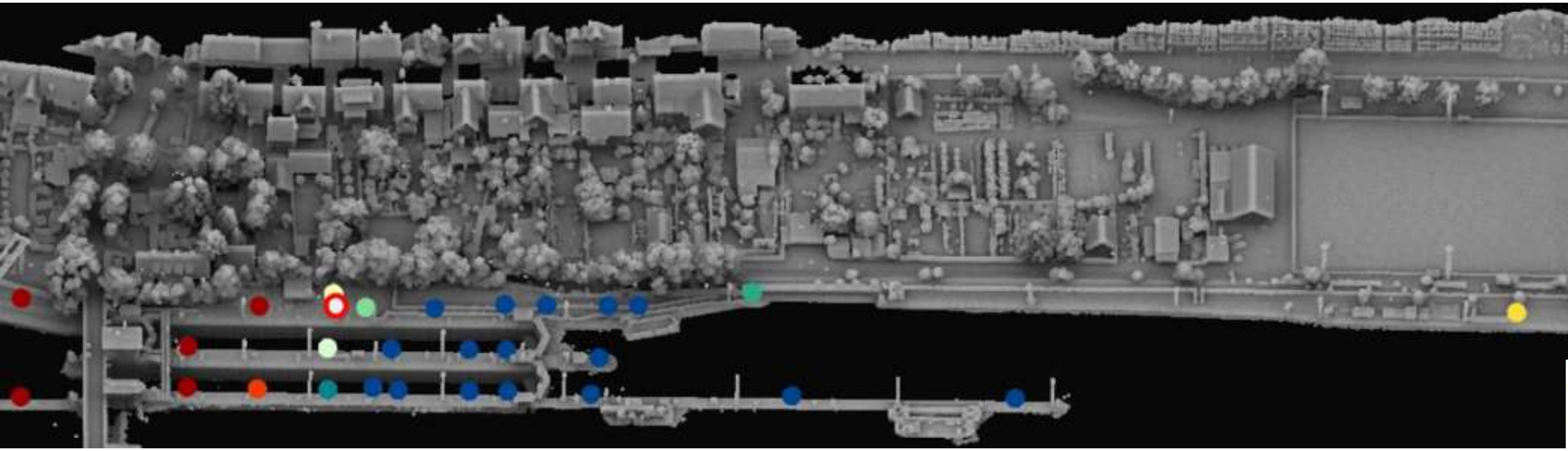

stand-alone LiDAR – image adjustment

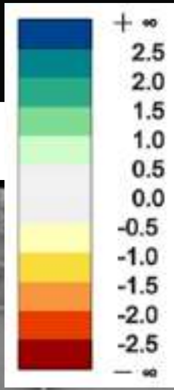

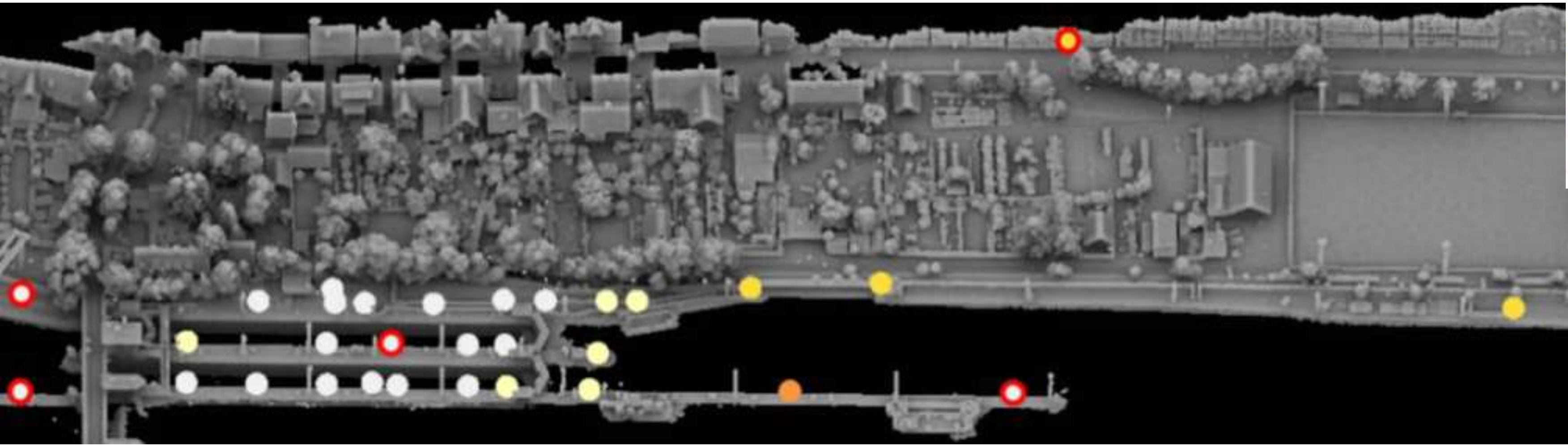

hybrid LiDAR – image adjustment

Bundle adjustment with raw inertial data

- typically GNSS/inertial data processing is done as pre-processing step before integrated sensor orientation
- this **approach fails in challenging scenarios**: short inertial/GNSS trajectories, weak photogrammetric block geometries, poor GNSS observations / signal quality
- **joint adjustment** of GNSS/inertial (**raw**) observations together with other sensors (camera / LiDAR) in **dynamic network / pose-graph optimization**

D. Cucci, M. Rehak & J. Skaloud (2017): Bundle adjustment with raw inertial observations in UAV applications, ISPRS Journal of Photogrammetry and Remote Sensing 130 (2017) 1–12
https://doi.org/10.1016/j.isprsjprs.2017.05.008

Bundle adjustment with raw inertial data

Processing chains in sensor orientation

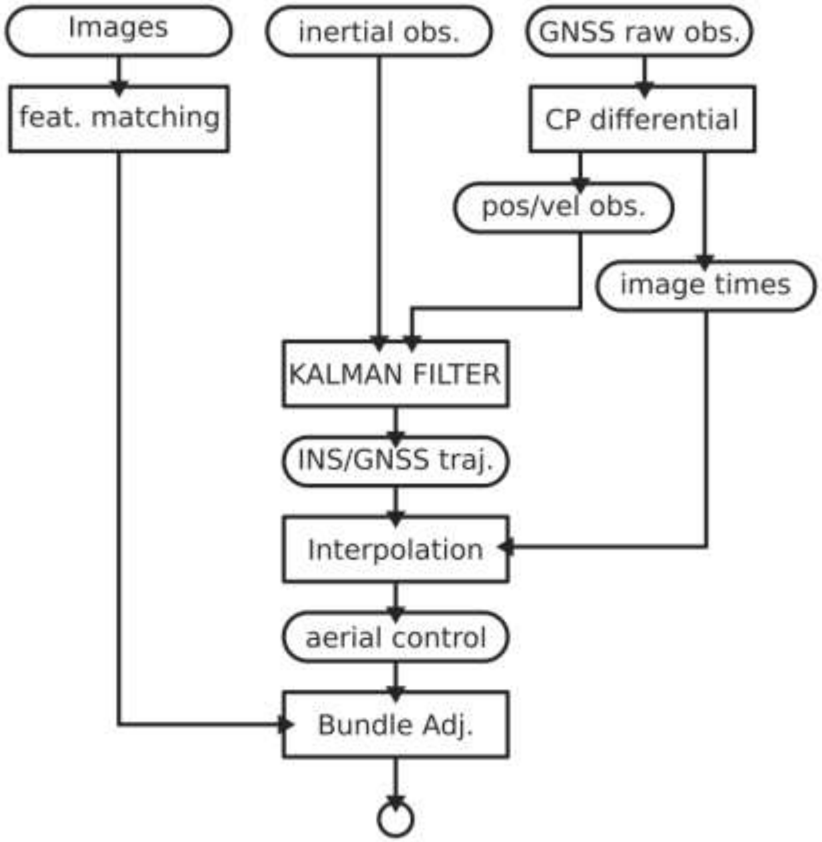

Traditional workflow

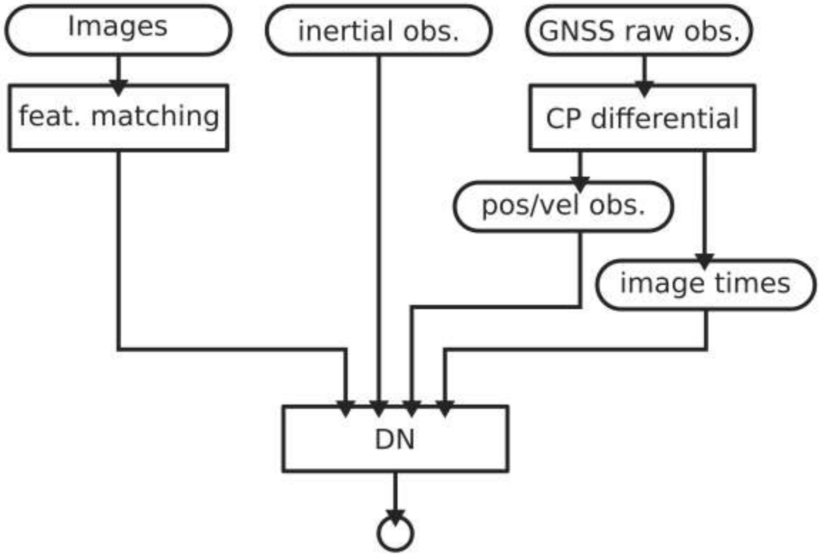

Modified workflow

Dynamic Networks – Integration of inertial raw data into sensor georeferencing

- determine the **navigation solution** (i.e., the trajectory), and, optionally, other parameters, such as inertial sensor biases, fusing all the available sensor readings **in a single step** ► **“tight fusion”** between inertial and image measurements.
- each “raw” sensor reading corresponds to an observation model, which forms the vector of unknowns:
  - Sensor poses (exterior orientations),
  - 3D position of the map-fixed features (object points) and
  - calibration parameters (interior orientation, boresight, lever-arms, IMU sensor biases)

- high number of unknowns because of high IMU rate has to be reduced (otherwise ill-conditioning), i.e. IMU pre-integration or solving through regularization

Dynamic Networks – Integration of inertial raw data into sensor georeferencing

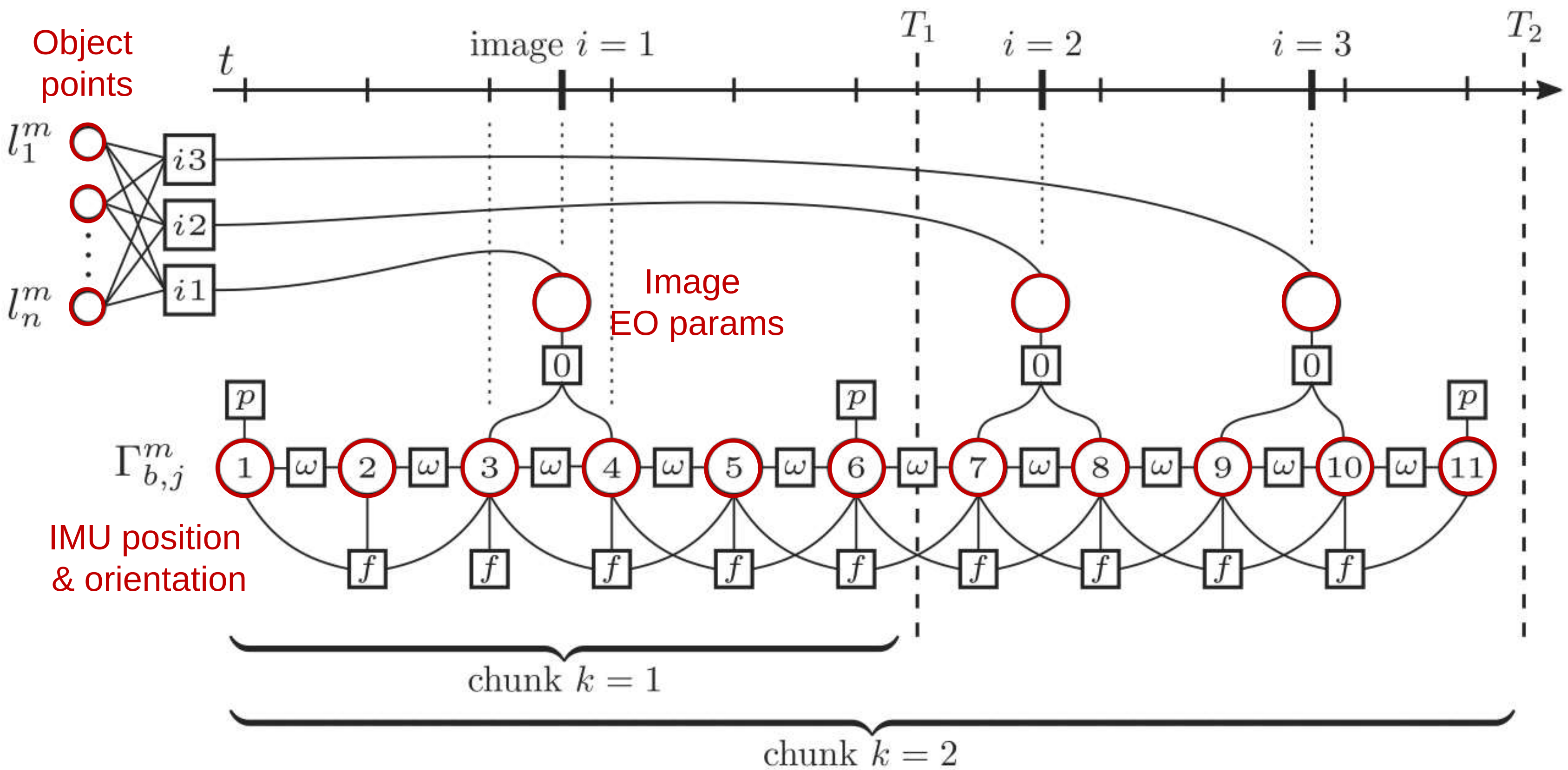

Dynamic Networks – Integration of inertial raw data into sensor georeferencing

Empirical UAV test flight – test layout

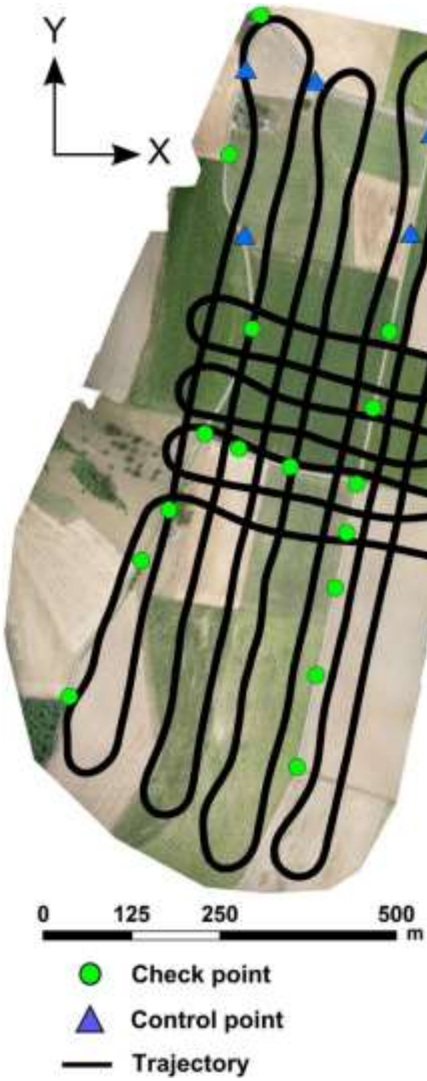

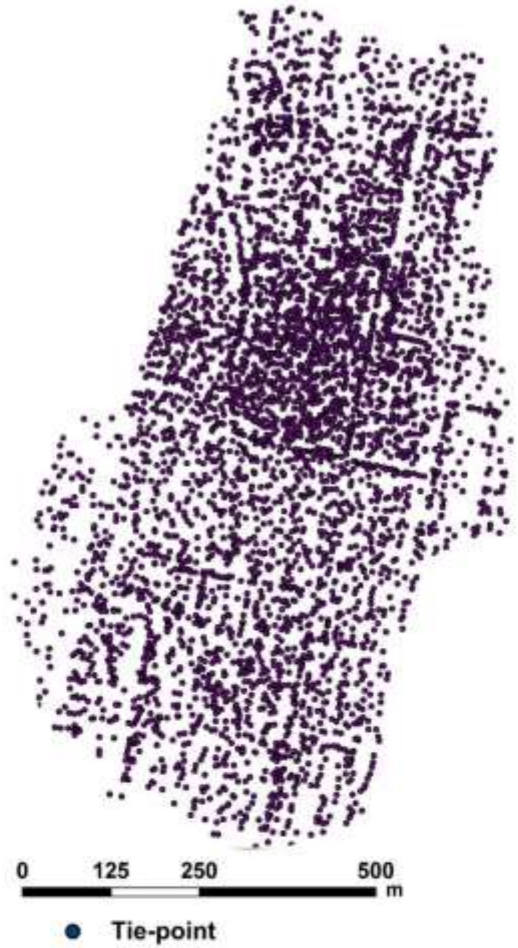

Remark: Data set already introduced before

© Cucci et al., 2017

Dynamic Networks – Integration of inertial raw data into sensor georeferencing

Empirical UAV test flight – tested scenarios

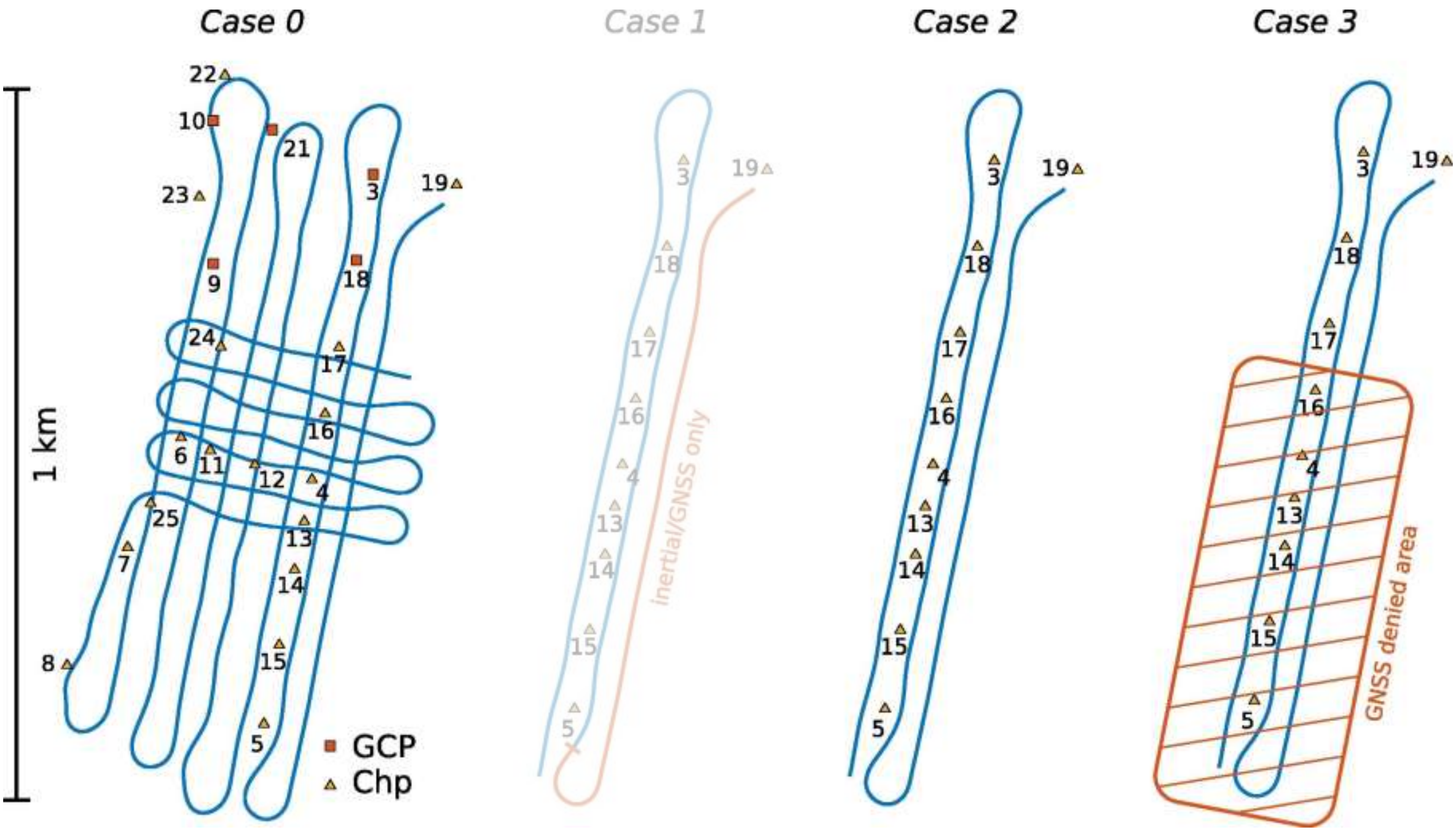

Dynamic Networks – Integration of inertial raw data into sensor georeferencing

Empirical UAV test flight – Case 0: Full photogrammetric block with GCP

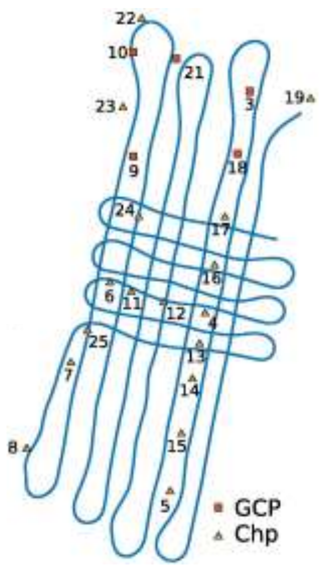

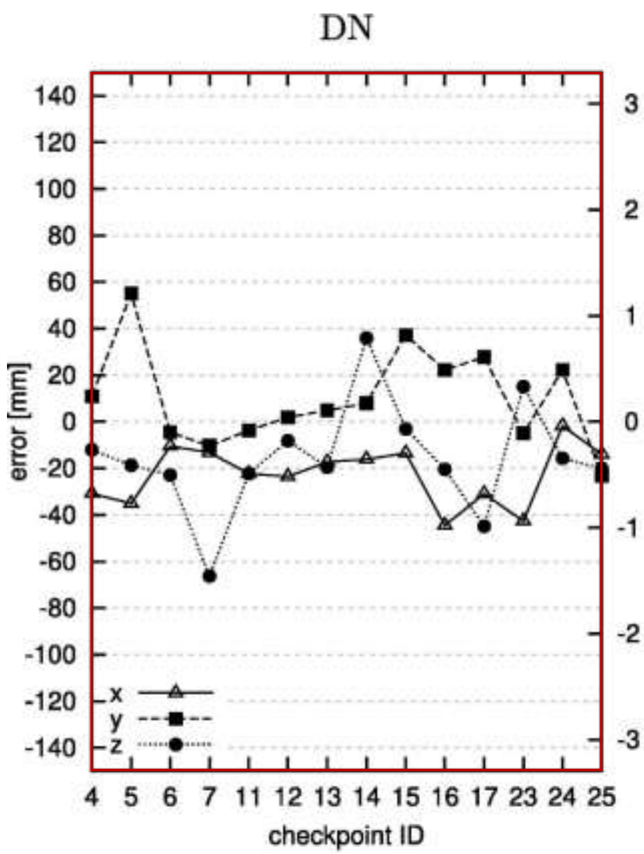

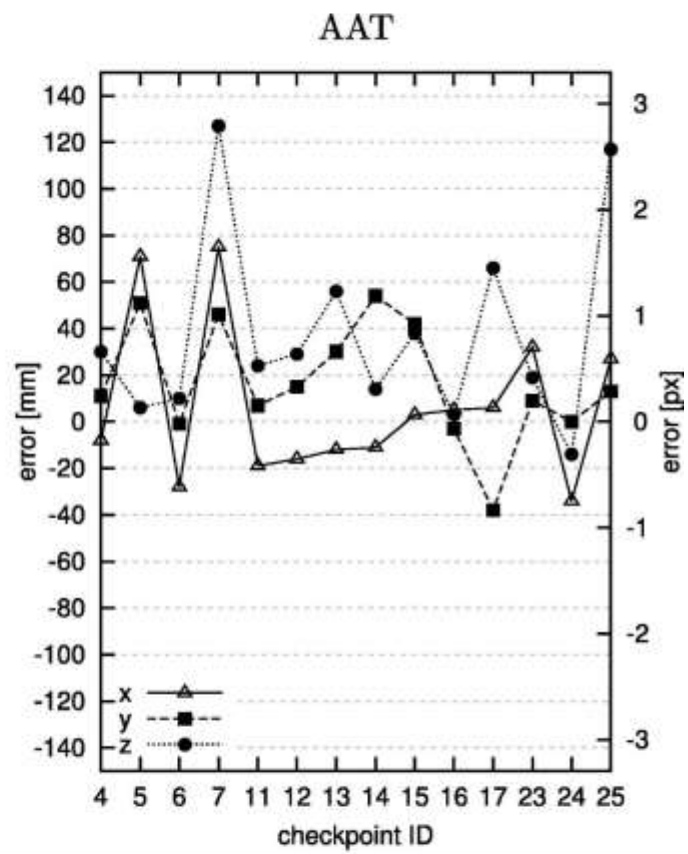

Check point residuals

	E	N	U
mean (mm)	−23	+10	−16
RMS (mm)	26	22	28

	E	N	U
mean (mm)	+6	+16	+35
RMS (mm)	32	29	53

Dynamic Networks – Integration of inertial raw data into sensor georeferencing

Empirical UAV test flight – Case 2: Corridor survey

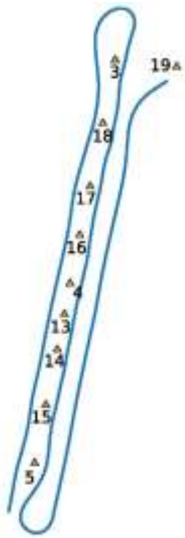

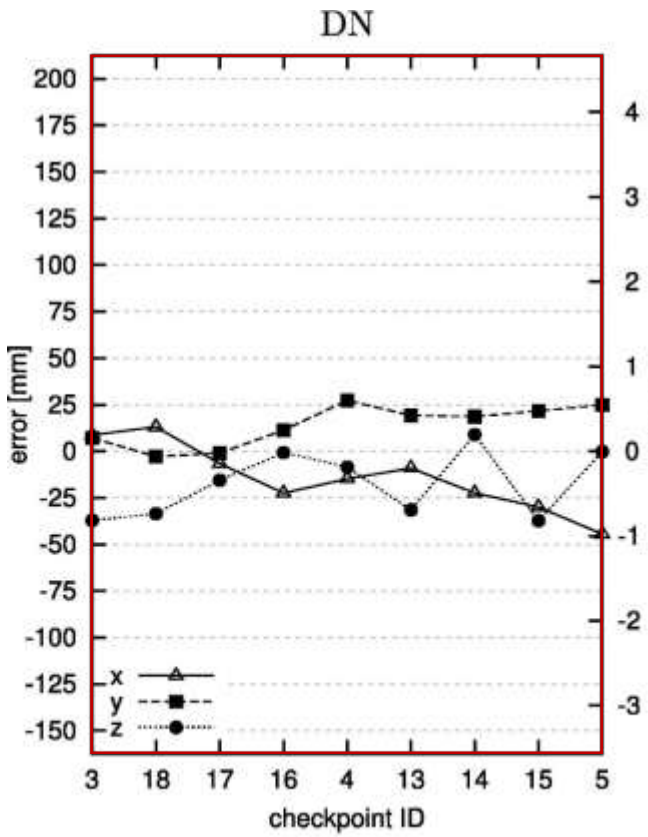

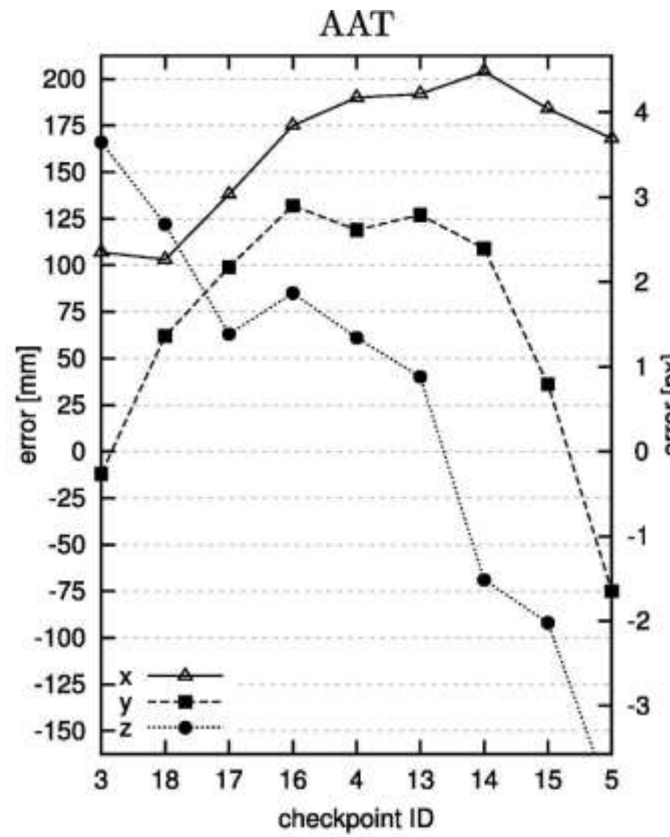

Check point residuals

	E	N	U
mean (mm)	−14	+14	−17
RMS (mm)	22	17	24

	E	N	U
mean (mm)	+160	+66	+12
RMS (mm)	164	95	108

Dynamic Networks – Integration of inertial raw data into sensor georeferencing

Empirical UAV test flight – Case 3: Corridor survey with GNSS blockages

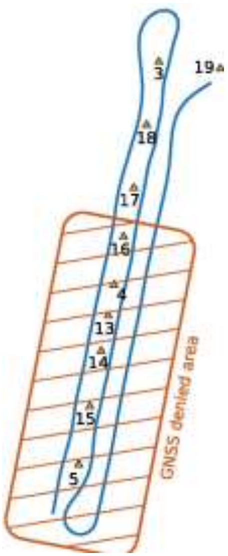

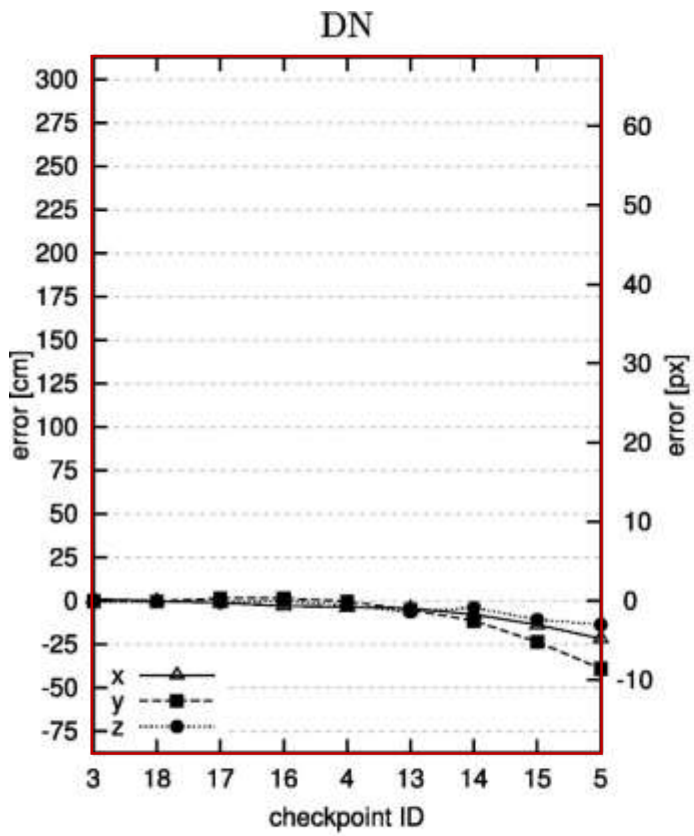

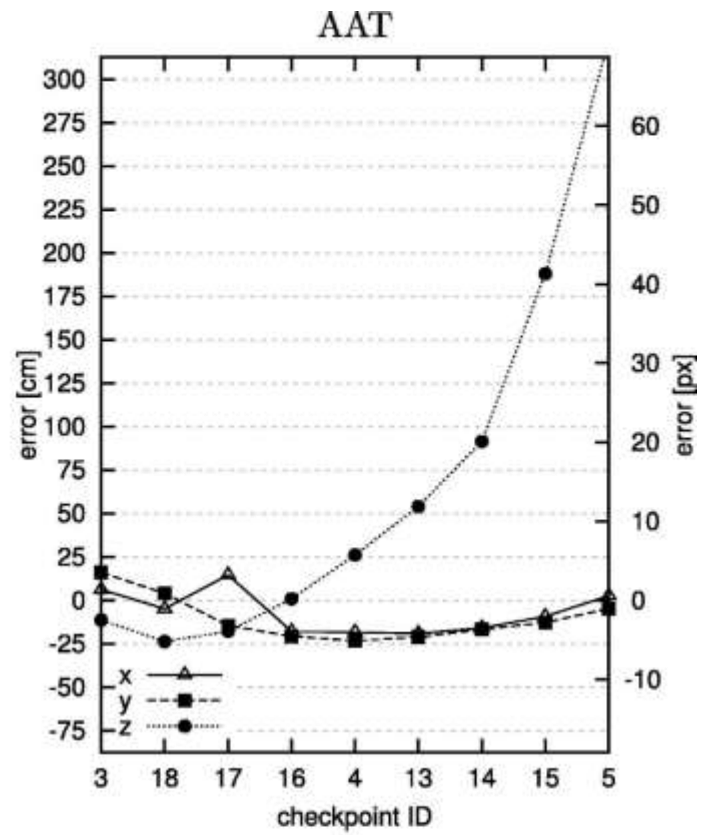

Check point residuals

DN:

	E	N	U
mean (mm)	−61	−86	−44
RMS (mm)	93	158	64

AAT:

	E	N	U
mean (mm)	−101	−104	+701
RMS (mm)	135	162	1301

Questions & Comments ?!

Universität Stuttgart
Institut für Photogrammetrie (ifp)

Tutorium DGPF Jahrestagung Stuttgart 2019
Institut für Photogrammetrie, Universität Stuttgart, 04.03.2020

ifp

Bibliography

- M. Blázquez & I. Colomina (2012): Relative INS/GNSS aerial control in integrated sensor orientation: Models and performance, in ISPRS Journal of Photogrammetry and Remote Sensing 67 (2012) 120–133 http://doi.org/10.1016/j.isprsjprs.2011.11.003
- M. Blázquez & I. Colomina (2012): Fast AT: A simple procedure for quasi direct orientation, in ISPRS Journal of Photogrammetry and Remote Sensing 71 (2012) 1–11, https://doi.org/10.1016/j.isprsjprs.2012.04.005
- D. Cucci, M. Rehak & J. Skaloud (2018): Bundle adjustment with raw inertial observations in UAV applications, ISPRS Journal of Photogrammetry and Remote Sensing, Volume 130, August 2017, Pages 1-12, https://doi.org/10.1016/j.isprsjprs.2017.05.008
- D. Cucci & J. Skaloud (2019): On raw inertial measurements in dynamic networks, ISPRS Ann. Photogramm. Remote Sens. Spatial Inf. Sci., IV-2/W5, 549-557, 2019, https://doi.org/10.5194/isprs-annals-IV-2-W5-549-2019

Bibliography

- P. Glira, N. Pfeifer, & G. Mandlburger: Hybrid orientation of airborne LiDAR point clouds and aerial images, ISPRS Ann. Photogramm. Remote Sens. Spatial Inf. Sci., IV-2/W5, 567-574, https://doi.org/10.5194/isprs-annals-IV-2-W5-567-2019, 2019
- Rehak, M. 2017: Integrated Sensor Orientation on micro aerial vehicles, Disseration at EPF Lausanne, Thesis No 7530, http://dx.doi.org/10.5075/epfl-thesis-7530
- Cramer, M.; Haala, N.; Laupheimer, D.; Mandlburger, G. & Havel, P. 2018: Ultra-high precision UAV-based LiDAR and Dense Image Matching. Int. Arch. Photogramm. Remote Sens. Spatial Inf. Sci., XLII-1, 115-120. DOI: 10.5194/isprs-archives-XLII-1-115-2018
- Cramer, M.; Mandlburger, G.; Laupheimer, D.; Haala, N. & Havel, P. 2019: Potenzial ultrahoch-auflösender und -genauer UAV-basierter 3D-Datenerfassung.– Publikationen der DGPF, Band 28, 2019, pp. 472-482. URL: https://www.dgpf.de/src/tagung/jt2019/proceedings/proceedings/papers/80_3LT2019_Cramer_et_al.pdf